

Models and Information Rates for Wiener Phase Noise Channels

Hassan Ghozlan and Gerhard Kramer, *Fellow, IEEE*

Abstract—A waveform channel is considered where the transmitted signal is corrupted by Wiener phase noise and additive white Gaussian noise. A discrete-time channel model that takes into account the effect of filtering on the phase noise is developed. The model is based on a multi-sample receiver, i.e., an integrate-and-dump filter whose output is sampled at a rate higher than the signaling rate. It is shown that, at high Signal-to-Noise Ratio (SNR), the multi-sample receiver achieves a rate that grows logarithmically with the SNR if the number of samples per symbol (oversampling factor) grows with the cubic root of the SNR. Moreover, the pre-log factor is at least 1/2 and can be achieved by amplitude modulation. Numerical simulations are used to compute lower bounds on the information rates achieved by the multi-sample receiver. The simulations show that oversampling is beneficial for both strong and weak phase noise at high SNR. In fact, the information rates are sometimes substantially larger than when using commonly-used approximate discrete-time models. Finally, for an approximate discrete-time model of the multi-sample receiver, the capacity pre-log at high SNR is at least 3/4 if the number of samples per symbol grows with the square root of the SNR. The analysis shows that phase modulation achieves a pre-log of at least 1/4 while amplitude modulation achieves a pre-log of 1/2. This is strictly greater than the capacity pre-log of the (approximate) discrete-time Wiener phase noise channel with only one sample per symbol, which is 1/2.

Index Terms—Phase noise, Wiener process, waveform channel, capacity, oversampling.

I. INTRODUCTION

Phase noise arises due to the instability of oscillators [1] in communication systems such as satellite communication [2], microwave links [3] or optical fiber communication [4]. The statistical characterization of the phase noise depends on the application. In systems with phase-locked loops (PLL), the residual phase noise follows a Tikhonov distribution [5]. In Digital Video Broadcasting DVB-S2, an example of a satellite communication system, the phase noise process is modeled by the sum of the outputs of two infinite-impulse response filters driven by the same white Gaussian noise process [2]. In optical

fiber communication, the phase noise in laser oscillators is modeled by a Wiener process [4].

A commonly studied *discrete-time* channel model is

$$Y_k = X_k e^{j\Theta_k} + Z_k \quad (1)$$

where $\{Y_k\}$ are the output symbols, $\{X_k\}$ are the input symbols, $\{\Theta_k\}$ is the phase noise process and $\{Z_k\}$ is additive white Gaussian noise (AWGN). For example, Katz and Shamai [6] studied the model (1) when $\{\Theta_k\}$ is independent and identically distributed (i.i.d.) according to $p_\Theta(\cdot)$, when Θ is uniformly distributed (called a non-coherent AWGN channel) and when Θ has a Tikhonov (or von Mises) distribution (called a partially-coherent AWGN channel). The i.i.d. Tikhonov phase noise models the residual phase error in systems with phase-tracking devices, e.g., phase-locked loops (PLL) and ideal interleavers/deinterleavers. Katz and Shamai [6] characterized some properties of the capacity-achieving distribution. Tight lower bounds on the capacities of memoryless non-coherent and partially coherent AWGN channels were computed by solving an optimization problem numerically in [6] and [7], respectively. Lapidoth studied in [8] a phase noise channel (1) at high SNR. He considered both memoryless phase noise and phase noise with memory. He showed that the capacity grows *logarithmically* with the SNR with a pre-log factor 1/2, where the pre-log is due to amplitude modulation only. The phase modulation contributes a bounded number of bits only. Dauwels and Loeliger [9] proposed a particle filtering method to compute information rates for discrete-time continuous-state channels with memory and applied the method to (1) for Wiener phase noise and auto-regressive-moving-average (ARMA) phase noise. Barletta, Magarini and Spalvieri [10] computed lower bounds on information rates for (1) with Wiener phase noise by using the auxiliary channel technique proposed in [11] and they computed upper bounds in [12]. They also developed a lower bound based on Kalman filtering in [13]. Barbieri and Colavolpe [14] computed lower bounds with an auxiliary channel slightly different from [10]. Capacity bounds are developed for a multi-input multi-output (MIMO) extension of the discrete-time model (1) in [15], [16].

A far less-studied model is the continuous-time model for phase noise channels, also called a *waveform* phase noise channel, see Fig. 1. The received waveform $r(t)$ is

$$r(t) = x(t) e^{j\theta(t)} + n(t), \text{ for } t \in \mathbb{R} \quad (2)$$

where $x(t)$ is the transmitted waveform while $n(t)$ and $\theta(t)$ are additive noise and phase noise, respectively. Continuous-time *white* phase noise was recently considered in [17, Section IV.C] and [18], [19]. We study the waveform channel (2) with *Wiener* phase noise. A detailed description of the channel is

The work of H. Ghozlan was supported by a USC Annenberg Fellowship and the National Science Foundation (NSF) under Grant CCF-09-05235. The work of G. Kramer was supported by an Alexander von Humboldt Professorship endowed by the German Federal Ministry of Education and Research, as well as by the NSF under Grant CCF-09-05235. Part of the material in this paper was presented at the IEEE International Symposium on Information Theory, Istanbul, Turkey, July, 2013, at the Global Communications Conference, Atlanta, GA, December, 2013 and at the IEEE International Symposium on Information Theory, Honolulu, HI, June/July, 2014.

H. Ghozlan is with the Department of Electrical Engineering, University of Southern California, Los Angeles, CA, 90089 USA (e-mail: ghozlan@usc.edu).

G. Kramer is with the Institute for Communications Engineering, Technische Universität München, 80333 Munich, Germany (email: gerhard.kramer@tum.de).

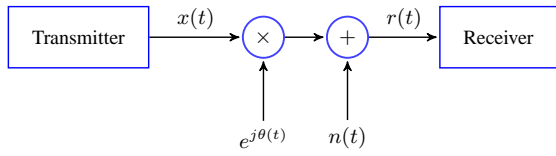


Fig. 1. Waveform phase noise channel.

given in Sec. II. This model is reasonable, for example, for optical fiber communication with low to intermediate power and laser phase noise, see [20]–[22]. Since the sampling of a continuous-time Wiener process yields a discrete-time Wiener process (Gaussian random walk), it is tempting to use the model (1) with $\{\Theta\}$ as a discrete-time Wiener process. However, this ignores the effect of *filtering* prior to sampling. It was pointed out in [20] that “even coherent systems relying on amplitude modulation (phase noise is obviously a problem in systems employing phase modulation) will suffer some degradation due to the presence of phase noise”. This is because the filtering converts phase fluctuations to amplitude variations. It is worth mentioning that filtering is necessary before sampling to limit the variance of the noise samples.

The model (1) thus does not fit the channel (2) and it is not obvious whether a pre-log 1/2 is achievable. The model that takes the effect of filtering into account is

$$Y_k = X_k H_k + N_k \quad (3)$$

where $\{H_k\}$ is a fading process. The model (3) falls in the class of non-coherent fading channels, i.e., the transmitter and receiver have knowledge of the distribution of the fading process $\{H_k\}$, but have no knowledge of its realization. For such channels, Lapidoth and Moser showed in [23] that, at high SNR, the capacity grows *double-logarithmically* with the SNR, when the process $\{H_k\}$ is stationary, ergodic, and *regular*.

Rather than using a filter and sampling its output at the symbol rate, we use a multi-sample receiver, i.e., a filter whose output is sampled many times per symbol. We show that this receiver achieves a rate that grows *logarithmically* with the SNR if the number of samples per symbol grows with the cubic root of the SNR. Furthermore, we show that a pre-log of 1/2 is achievable through amplitude modulation. We also show for an approximate multi-sample model that phase modulation contributes 1/4 to the pre-log factor at high SNR, if the oversampling factor grows with the square root of SNR. We corroborate the results of the high-SNR analysis with numerical simulations at finite SNR. This paper collects and extends results presented in [24]–[26].

Benefits of oversampling were reported for other problems. For example, in some digital storage systems, it was shown by numerical simulations that oversampling can increase the information rate [27]. In a low-pass-filter-and-limiter (nonlinear) channel, it was found that oversampling (with a factor of 2) offers a higher information rate [28]. It was demonstrated in [29] that doubling the sampling rate recovers some of the loss in capacity incurred on the bandlimited Gaussian channel with a one-bit output quantizer. For non-coherent block fading channels, it was shown in [30] that by doubling the sampling

rate the information rate grows logarithmically at high SNR with a pre-log $1 - 1/N$ rather than $1 - Q/N$ which is the pre-log achieved by sampling at symbol rate (N is the length of the fading block and Q is the rank of the covariance matrix of the discrete-time channel gains within each block).

This paper is organized as follows. The continuous-time model is described in Sec. II and the discrete-time models of the matched filter receiver and the multi-sample receiver are described in Sec. III. We derive a lower bound on the capacity in Sec. IV based on amplitude modulation and show that the pre-log factor is at least 1/2 if the oversampling factor grows with the cubic root of the SNR. We develop algorithms to compute tight lower bounds on the information rates of a multi-sample receiver in Sec. V. In Sec. VI, we report the results of numerical simulations which demonstrate the importance of increasing the oversampling factor with the SNR to achieve higher rates. We derive a lower bound on the rate achieved by phase modulation for an approximate multi-sample discrete-time model in Sec. VII and we show that phase modulation contributes at least 1/4 to the pre-log factor, resulting in an overall pre-log factor of 3/4 when both amplitude and phase modulation are used. This is achieved by using an oversampling factor that grows with the square root of the SNR. In Sec. VIII, we summarize our results and mention some open problems. Finally, we conclude with Sec. IX.

II. WAVEFORM PHASE NOISE CHANNEL

We use the following notation: $j = \sqrt{-1}$, $*$ denotes the complex conjugate, δ_D is the Dirac delta function, $\lceil \cdot \rceil$ is the ceiling operator. We use X^k as a shorthand for (X_1, X_2, \dots, X_k) . Suppose the transmit-waveform is $x(t)$ and the receiver observes

$$r(t) = x(t) e^{j\theta(t)} + n(t) \quad (4)$$

where $n(t)$ is a realization of a white circularly-symmetric complex Gaussian process $N(t)$ with

$$\begin{aligned} \mathbb{E}[N(t)] &= 0 \\ \mathbb{E}[N(t_1)N^*(t_2)] &= \sigma_N^2 \delta_D(t_2 - t_1). \end{aligned} \quad (5)$$

The phase $\theta(t)$ is a realization of a Wiener process $\Theta(t)$:

$$\Theta(t) = \Theta(0) + \int_0^t W(\tau) d\tau \quad (6)$$

where $\Theta(0)$ is uniform on $[-\pi, \pi)$ and $W(t)$ is a real Gaussian process with

$$\begin{aligned} \mathbb{E}[W(t)] &= 0 \\ \mathbb{E}[W(t_1)W(t_2)] &= 2\pi\beta \delta_D(t_2 - t_1). \end{aligned} \quad (7)$$

The processes $N(t)$ and $\Theta(t)$ are independent of each other and independent of the input. $N_0 = 2\sigma_N^2$ is the single-sided power spectral density of the additive noise. We define $U(t) \equiv \exp(j\Theta(t))$. The auto-correlation function of $U(t)$ is

$$R_U(t_1, t_2) = \mathbb{E}[U(t_1)U^*(t_2)] = \exp(-\pi\beta|t_2 - t_1|) \quad (8)$$

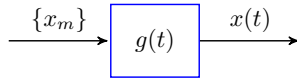


Fig. 2. Transmitter: pulse-shaping filter.

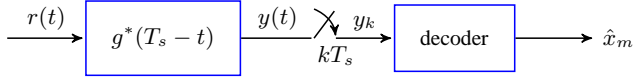


Fig. 3. Matched filter receiver with symbol rate sampling.

and the power spectral density of $U(t)$ is

$$S_U(f) = \int_{-\infty}^{\infty} R_U(t, t + \tau) e^{-j2\pi f\tau} d\tau = \frac{1}{\pi} \frac{\beta/2}{(\beta/2)^2 + f^2}. \quad (9)$$

The spectrum is said to have a Lorentzian shape. We have $\beta = f_{\text{FWHM}} = 2f_{\text{HWHM}}$ where f_{FWHM} is the full-width at half-maximum and f_{HWHM} is the half-width at half-maximum.

Let T be the transmission interval, then the transmitted waveforms must satisfy the power constraint

$$\mathbb{E} \left[\frac{1}{T} \int_0^T |X(t)|^2 dt \right] \leq \mathcal{P} \quad (10)$$

where $X(t)$ is a random process whose realization is $x(t)$.

III. DISCRETE-TIME MODELS

A. Transmitter

Let (x_1, x_2, \dots, x_b) be the codeword sent by the transmitter. Suppose the transmitter uses a unit-energy pulse $g(t)$ whose time support is $[0, T_s]$ where T_s is the symbol interval (see Fig. 2). The waveform sent by the transmitter is

$$x(t) = \sum_{m=1}^b x_m g(t - (m-1)T_s). \quad (11)$$

B. Matched Filter Receiver

The received signal $r(t)$ is fed to a matched filter and the output $y(t)$ of the filter is sampled at symbol rate (also called Baud rate) as illustrated in Fig. 3. The k -th output sample is

$$\begin{aligned} y_k &= r(t) \star g^*(T_s - t)|_{t=kT_s} \\ &= x_k \int_{-\infty}^{\infty} e^{j\theta(\tau)} |g(\tau - (k-1)T_s)|^2 d\tau + n_k \end{aligned} \quad (12)$$

where $k = 1, \dots, b$, \star denotes convolution and n_k is the part of the output due to the additive noise. Therefore, we have the discrete-time model

$$Y_k = X_k H_k + N_k \quad (13)$$

where

$$H_k \equiv \int_{-\infty}^{\infty} e^{j\theta(\tau)} |g(\tau - (k-1)T_s)|^2 d\tau. \quad (14)$$

The transmitter and receiver know the distribution of the fading process $\{H_k\}$ but have no knowledge of its realization. For this model, Lapidoth and Moser showed in [23] that, at high

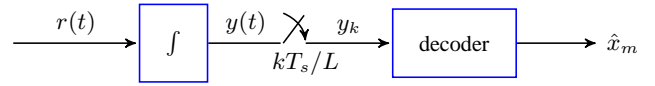


Fig. 4. Multi-sample receiver.

SNR, the capacity grows *double-logarithmically* with the SNR when the process $\{H_k\}$ is stationary, ergodic, and *regular*.

A commonly-used approximation for H_k is

$$\begin{aligned} &\int_{-\infty}^{\infty} e^{j\theta(\tau)} |g(\tau - (k-1)T_s)|^2 d\tau \\ &\approx e^{j\theta(kT_s)} \int_{-\infty}^{\infty} |g(\tau - (k-1)T_s)|^2 d\tau \end{aligned}$$

which yields the approximate discrete-time model

$$Y_k = X_k e^{j\theta(kT_s)} + N_k. \quad (15)$$

C. Multi-sample Receiver

Consider next a multi-sample receiver (see Fig. 4). Let L be the number of samples per symbol ($L \geq 1$) and define the sample interval as

$$\Delta = \frac{T_s}{L}. \quad (16)$$

The received waveform $r(t)$ is filtered using an integrator over a sample interval to give the output signal

$$y(t) = \int_{t-\Delta}^t r(\tau) d\tau. \quad (17)$$

The signal $y(t)$ is a realization of a random process $Y(t)$ that is sampled at $t = k\Delta$, $k = 1, \dots, n = bL$. Hence, we have the discrete-time model in which the k -th output sample is

$$Y_k = X_{\lceil k/L \rceil} \Delta e^{j\Theta_k} F_k + N_k \quad (18)$$

where $Y_k \equiv Y(k\Delta)$, $\Theta_k \equiv \Theta((k-1)\Delta)$,

$$F_k \equiv \frac{1}{\Delta} \int_{(k-1)\Delta}^{k\Delta} g\left(\tau - \left(\left\lceil \frac{k}{L} \right\rceil - 1\right)T_s\right) e^{j(\Theta(\tau) - \Theta_k)} d\tau \quad (19)$$

and

$$N_k \equiv \int_{(k-1)\Delta}^{k\Delta} N(\tau) d\tau. \quad (20)$$

The process $\{N_k\}$ is an i.i.d. circularly-symmetric complex Gaussian process with

$$\mathbb{E}[N_k] = 0 \quad (21)$$

$$\mathbb{E}[N_k N_\ell^*] = \sigma_N^2 \Delta \delta_K[\ell - k] \quad (22)$$

$$\mathbb{E}[N_k N_\ell] = 0 \quad (23)$$

where $\delta_K[\cdot]$ is the Kronecker delta. The process $\{\Theta_k\}$ is the discrete-time Wiener process:

$$\Theta_k = \Theta_{k-1} + W_k \quad (24)$$

for $k = 2, \dots, n$, where Θ_1 is uniform on $[-\pi, \pi)$ and $\{W_k\}$ is an i.i.d. real Gaussian process with mean 0 and $\mathbb{E}[W_k^2] =$

$2\pi\beta\Delta$, i.e., the probability density function (pdf) of W_k is $p_{W_k}(w) = G(w; 0, \sigma_W^2)$ where

$$G(w; \mu, \sigma^2) = \frac{1}{\sqrt{2\pi\sigma^2}} \exp\left(-\frac{(w-\mu)^2}{2\sigma^2}\right) \quad (25)$$

and $\sigma_W^2 = 2\pi\beta\Delta$. The random variable $(W_k \bmod 2\pi)$ is a *wrapped Gaussian* and its pdf is

$$p_W(w; \sigma^2) = \sum_{i=-\infty}^{\infty} G(w - 2i\pi; 0, \sigma^2). \quad (26)$$

Moreover, $\{F_k\}$ and $\{W_k\}$ are independent of $\{N_k\}$ but not independent of each other. Equations (10) and (11) imply the power constraint

$$\frac{1}{b} \sum_{m=1}^b \mathbb{E}[|X_m|^2] \leq P \equiv \mathcal{P}T_s. \quad (27)$$

The signal-to-noise ratio SNR is defined as

$$\text{SNR} \equiv \frac{P}{\sigma_N^2 T_s} = \frac{\mathcal{P}}{\sigma_N^2}. \quad (28)$$

IV. HIGH SNR

In this section, we study rectangular pulses, i.e., we consider

$$g(t) \equiv \begin{cases} \sqrt{1/T_s}, & 0 \leq t < T_s, \\ 0, & \text{otherwise.} \end{cases} \quad (29)$$

It follows that F_k in (19) becomes

$$F_k \equiv \frac{1}{\Delta} \int_{(k-1)\Delta}^{k\Delta} e^{j(\Theta(\tau) - \Theta_k)} d\tau. \quad (30)$$

The process $\{F_k\}$ is i.i.d. (see Appendix A.1). For the k th input symbol, we have L outputs, so it is convenient to group the L samples per symbol in one vector

$$\mathbf{Y}_k \equiv (Y_{(k-1)L+1}, Y_{(k-1)L+2}, \dots, Y_{(k-1)L+L}). \quad (31)$$

We use \mathbf{Y}^k as a shorthand for $(\mathbf{Y}_1, \mathbf{Y}_2, \dots, \mathbf{Y}_k)$. The capacity of a point-to-point channel is given by

$$C(\text{SNR}) = \lim_{b \rightarrow \infty} \frac{1}{b} \sup I(X^b; \mathbf{Y}^b) \quad (32)$$

where the supremum is over all joint distributions of the input symbols satisfying the power constraint. For a given input distribution, the achievable rate R is

$$R(\text{SNR}) = I(X; \mathbf{Y}) \equiv \lim_{b \rightarrow \infty} \frac{1}{b} I(X^b; \mathbf{Y}^b). \quad (33)$$

We define $X_A \equiv |X|$ and $\Phi_X \equiv \angle X$ where \angle denotes the phase angle (also called the argument) of a complex number. We decompose the mutual information using the chain rule into two parts:

$$I(X^b; \mathbf{Y}^b) = I(X_A^b; \mathbf{Y}^b) + I(\Phi_X^b; \mathbf{Y}^b | X_A^b). \quad (34)$$

Define

$$I(X_A; \mathbf{Y}) \equiv \lim_{b \rightarrow \infty} \frac{1}{b} I(X_A^b; \mathbf{Y}^b) \quad (35)$$

and

$$I(\Phi_X; \mathbf{Y} | X_A) \equiv \lim_{b \rightarrow \infty} \frac{1}{b} I(\Phi_X^b; \mathbf{Y}^b | X_A^b). \quad (36)$$

It follows from (33)–(36) that

$$I(X; \mathbf{Y}) = I(X_A; \mathbf{Y}) + I(\Phi_X; \mathbf{Y} | X_A). \quad (37)$$

The first term represents the contribution of the amplitude modulation while the second term represents the contribution of the phase modulation.

A. Amplitude Modulation

Consider first the contribution of amplitude modulation. Suppose that X_A^b is i.i.d. so that

$$\begin{aligned} I(X_A^b; \mathbf{Y}^b) &\stackrel{(a)}{=} \sum_{k=1}^b I(X_{A,k}; \mathbf{Y}^b | X_A^{k-1}) \\ &\stackrel{(b)}{=} \sum_{k=1}^b H(X_{A,k}) - H(X_{A,k} | \mathbf{Y}^b X_A^{k-1}) \\ &\stackrel{(c)}{\geq} \sum_{k=1}^b I(X_{A,k}; \mathbf{Y}_k) \\ &\stackrel{(d)}{\geq} \sum_{k=1}^b I(X_{A,k}; V_k) \end{aligned} \quad (38)$$

where

$$V_k = \sum_{\ell=1}^L |Y_{(k-1)L+\ell}|^2. \quad (39)$$

Step (a) follows from the chain rule of mutual information, (b) follows from the independence of $X_{A,1}, X_{A,2}, \dots, X_{A,n}$, (c) holds because conditioning does not increase entropy, and (d) follows from the data processing inequality. Since X_A^b is identically distributed, then V^b is also identically distributed and we have, for $k \geq 2$,

$$I(X_{A,k}; V_k) = I(X_{A,1}; V_1). \quad (40)$$

In the rest of this section, we consider only one symbol ($k = 1$) and drop the time index. Moreover, we set $T_s = 1$ for simplicity. By combining (39) and (18), we have

$$\begin{aligned} V &= \sum_{\ell=1}^L (X_A^2 \Delta^2 |F_\ell|^2 + 2X_A \Delta \Re[e^{j\Phi_X} e^{j\Theta_\ell} F_\ell N_\ell^*] + |N_\ell|^2) \\ &= X_A^2 \Delta G + 2X_A \Delta Z_1 + Z_0 \end{aligned} \quad (41)$$

where G , Z_1 and Z_0 are defined as

$$G \equiv \frac{1}{L} \sum_{\ell=1}^L |F_\ell|^2 \quad (42)$$

$$Z_1 \equiv \sum_{\ell=1}^L \Re[e^{j\Phi_X} e^{j\Theta_\ell} F_\ell N_\ell^*] \quad (43)$$

$$Z_0 \equiv \sum_{\ell=1}^L |N_\ell|^2. \quad (44)$$

The second-order statistics of Z_1 and Z_0 are (see Appendix A.2)

$$\begin{aligned} \mathbb{E}[Z_1] &= 0 & \text{Var}[Z_1] &= \mathbb{E}[G] \sigma_N^2 / 2 \\ \mathbb{E}[Z_0] &= \sigma_N^2 & \text{Var}[Z_0] &= \sigma_N^4 \Delta \\ \mathbb{E}[Z_1(Z_0 - \mathbb{E}[Z_0])] &= 0. \end{aligned} \quad (45)$$

By using the Auxiliary-Channel Lower Bound Theorem in [11, Sec. VI], we have

$$I(X_A; V) \geq \mathbb{E}[-\log q_V(V)] - \mathbb{E}[-\log q_{V|X_A}(V|X_A)] \quad (46)$$

where $q_{V|X_A}(v|x_A)$ is an arbitrary auxiliary channel and

$$q_V(v) = \int p_{X_A}(x_A) q_{V|X_A}(v|x_A) dx_A \quad (47)$$

where $p_{X_A}(\cdot)$ is the *true* input pdf, i.e., $q_V(\cdot)$ is the output pdf obtained by connecting the true input source to the auxiliary channel. Note that $\mathbb{E}[\cdot]$ is the expectation according to the *true* distribution of X_A and V . We point out that any auxiliary channel gives a valid lower bound; the ‘‘closer’’ the auxiliary channel is to the true channel, the tighter the lower bound. We choose the auxiliary channel

$$V^{\text{auxiliary}} = X_A^2 \Delta \tilde{G} + 2X_A \Delta \tilde{Z}_1 + \tilde{Z}_0 \quad (48)$$

where \tilde{G} , \tilde{Z}_1 and \tilde{Z}_0 are defined as

$$\tilde{G} \equiv 1 \quad (49)$$

$$\tilde{Z}_1 \equiv \sum_{\ell=1}^L \Re[e^{j\Phi_\ell} e^{j\Theta_\ell} N_\ell^*] \quad (50)$$

$$\tilde{Z}_0 \equiv \sigma_N^2. \quad (51)$$

We make a few remarks to motivate our choice of the auxiliary channel:

- G converges to 1 (in mean square) as $L \rightarrow \infty$ (see (219) in Appendix A.4).
- Since N_ℓ is circularly-symmetric complex Gaussian, then $e^{j\Phi_\ell} e^{j\Theta_\ell} N_\ell^*$ is also circularly-symmetric complex Gaussian with the same variance of N_ℓ . It follows that \tilde{Z}_1 is Gaussian since it is a linear combination of Gaussian random variables. More specifically, the random variable \tilde{Z}_1 is Gaussian with mean zero and variance $\sigma_N^2/2$. In addition, Z_1 converges to \tilde{Z}_1 (in mean square) as $L \rightarrow \infty$. This can be shown by computing (using steps similar to (192) in Appendix A.2)

$$\mathbb{E}[|Z_1 - \tilde{Z}_1|^2] = \frac{1}{2} \sigma_N^2 \Delta L \mathbb{E}[|F_1 - 1|^2] \quad (52)$$

and using (215) in Appendix A.3 to get

$$\lim_{L \rightarrow \infty} \mathbb{E}[|Z_1 - \tilde{Z}_1|^2] = \frac{1}{2} \sigma_N^2 \lim_{a \rightarrow 1} \mathbb{E}[|F_1 - 1|^2] = 0. \quad (53)$$

- Z_0 converges to σ_N^2 (in mean square) as $L \rightarrow \infty$. This follows directly by taking the limit of $\text{Var}(Z_0)$ given in (45):

$$\lim_{L \rightarrow \infty} \mathbb{E}[(Z_0 - \sigma_N^2)^2] = \lim_{\Delta \rightarrow 0} \sigma_N^4 \Delta = 0. \quad (54)$$

In summary, the conditional distribution $q_{V|X_A}$ of the auxiliary channel is

$$q_{V|X_A}(v|x_A) = \frac{1}{\sqrt{4\pi x_A^2 \Delta^2 \sigma_N^2}} \exp\left(-\frac{(v - x_A^2 \Delta - \sigma_N^2)^2}{4x_A^2 \Delta^2 \sigma_N^2}\right). \quad (55)$$

It follows that

$$\begin{aligned} \mathbb{E}[-\log(q_{V|X_A}(V|X_A))] &= \mathbb{E}\left[\frac{(V - X_A^2 \Delta - \sigma_N^2)^2}{4X_A^2 \Delta^2 \sigma_N^2}\right] \\ &+ \log \Delta + \frac{1}{2} \log(4\pi \sigma_N^2) + \frac{1}{2} \mathbb{E}[\log(X_A^2)]. \end{aligned} \quad (56)$$

By using (41), we have

$$\begin{aligned} &(V - X_A^2 \Delta - \sigma_N^2)^2 \\ &= (X_A^2 \Delta (G - 1) + 2X_A \Delta Z_1 + (Z_0 - \sigma_N^2))^2 \\ &= X_A^4 \Delta^2 (G - 1)^2 + 4X_A^2 \Delta^2 Z_1^2 + (Z_0 - \sigma_N^2)^2 \\ &+ 4X_A^3 \Delta^2 (G - 1)Z_1 + 2X_A^2 \Delta (G - 1)(Z_0 - \sigma_N^2) \\ &+ 4X_A \Delta Z_1 (Z_0 - \sigma_N^2) \end{aligned} \quad (57)$$

and hence, by using (45), we have

$$\begin{aligned} &\mathbb{E}\left[\frac{(V - X_A^2 \Delta - \sigma_N^2)^2}{4X_A^2 \Delta^2 \sigma_N^2}\right] \\ &= \frac{1}{4\sigma_N^2} \mathbb{E}[X_A^2] \mathbb{E}[(G - 1)^2] + \frac{1}{\sigma_N^2} \mathbb{E}[Z_1^2] \\ &+ \frac{1}{4\Delta^2 \sigma_N^2} \mathbb{E}\left[\frac{1}{X_A^2}\right] \mathbb{E}[(Z_0 - \sigma_N^2)^2] + \frac{1}{\sigma_N^2} \mathbb{E}[X_A] \mathbb{E}[(G - 1)Z_1] \\ &+ \frac{1}{2\Delta \sigma_N^2} \mathbb{E}[G - 1] \mathbb{E}[Z_0 - \sigma_N^2] + \frac{1}{\Delta \sigma_N^2} \mathbb{E}\left[\frac{1}{X_A}\right] \mathbb{E}[Z_1(Z_0 - \sigma_N^2)] \\ &= \frac{1}{4\sigma_N^2} P \mathbb{E}[(G - 1)^2] + \frac{1}{2} \mathbb{E}[G] + \frac{\sigma_N^2}{4\Delta} \mathbb{E}\left[\frac{1}{X_A^2}\right] \end{aligned} \quad (58)$$

where we also used (see Appendix A.2)

$$\mathbb{E}[(G - 1)Z_1] = 0. \quad (59)$$

Substituting (58) into (56) and using $\mathbb{E}[G] \leq 1$ yield

$$\begin{aligned} &\mathbb{E}[-\log(q_{V|X_A}(V|X_A))] \\ &\leq \log \Delta + \frac{1}{2} \log(4\pi \sigma_N^2) + \frac{1}{2} \mathbb{E}[\log(X_A^2)] \\ &+ \frac{P}{4\sigma_N^2} \mathbb{E}[(G - 1)^2] + \frac{1}{2} + \frac{\sigma_N^2}{4\Delta} \mathbb{E}\left[\frac{1}{X_A^2}\right]. \end{aligned} \quad (60)$$

It is convenient to define $X_P \equiv X_A^2$. We choose the input distribution

$$p_{X_P}(x_P) = \begin{cases} \frac{1}{\lambda} \exp\left(-\frac{x_P - P_{\min}}{\lambda}\right), & x_P \geq P_{\min} \\ 0, & \text{otherwise} \end{cases} \quad (61)$$

where $0 < P_{\min} < P$ and $\lambda = P - P_{\min}$, so that

$$\mathbb{E}[X_P] = \mathbb{E}[X_A^2] = P. \quad (62)$$

It follows from (47) and (61) that

$$\begin{aligned} q_V(v) &= \int_{P_{\min}}^{\infty} \frac{1}{\lambda} \exp\left(-\frac{x_P - P_{\min}}{\lambda}\right) q_{V|X_P}(v|x_P) dx_P \\ &\leq \exp(P_{\min}/\lambda) F_V(v) \end{aligned} \quad (63)$$

where

$$q_{V|X_P}(v|x_P) = q_{V|X_A}(v|\sqrt{x_P}) \quad (64)$$

and

$$f_V(v) \equiv \int_0^{\infty} \frac{1}{\lambda} \exp\left(-\frac{x_P}{\lambda}\right) q_{V|X_P}(v|x_P) dx_P. \quad (65)$$

The inequality (63) follows from the non-negativity of the integrand. By combining (55), (64), (65) and making the change of variables $x = x_P \Delta$, we have

$$\begin{aligned} f_V(v) &= \int_0^\infty \frac{e^{-x/(\lambda\Delta)}}{\lambda\Delta} \frac{1}{\sqrt{4\pi x\Delta\sigma_N^2}} \exp\left(-\frac{(v-x-\sigma_N^2)^2}{4x\Delta\sigma_N^2}\right) dx \\ &= \frac{1}{\sqrt{\lambda\Delta(\lambda\Delta + 4\Delta\sigma_N^2)}} \times \\ &\quad \exp\left(\frac{2}{4\Delta\sigma_N^2} \left[v - \sigma_N^2 - |v - \sigma_N^2| \sqrt{1 + \frac{4\Delta\sigma_N^2}{\lambda\Delta}} \right]\right) \end{aligned} \quad (66)$$

where we used equation (140) in Appendix A of [31]:

$$\begin{aligned} &\int_0^\infty \frac{1}{a} \exp\left(-\frac{x}{a}\right) \frac{1}{\sqrt{\pi bx}} \exp\left(-\frac{(u-x)^2}{bx}\right) dx \\ &= \frac{1}{\sqrt{a(a+b)}} \exp\left(\frac{2}{b} \left[u - |u| \sqrt{1 + \frac{b}{a}} \right]\right). \end{aligned} \quad (67)$$

Therefore, we have

$$\begin{aligned} &\mathbb{E}[-\log(f_V(V))] \\ &= \frac{1}{2} \log(\Delta^2(\lambda^2 + 4\lambda\sigma_N^2)) \\ &\quad - \frac{1}{2\Delta\sigma_N^2} \left[\mathbb{E}[V - \sigma_N^2] - \mathbb{E}[|V - \sigma_N^2|] \sqrt{1 + \frac{4\sigma_N^2}{\lambda}} \right] \\ &\stackrel{(a)}{\geq} \log(\Delta\lambda) + \frac{1}{2\sigma_N^2\Delta} \mathbb{E}[V - \sigma_N^2] \left[\sqrt{1 + \frac{4\sigma_N^2}{\lambda}} - 1 \right] \\ &\stackrel{(b)}{\geq} \log(\Delta\lambda) \end{aligned} \quad (68)$$

where (a) holds because the logarithmic function is monotonic and $\mathbb{E}[|\cdot|] \geq \mathbb{E}[\cdot]$, and (b) holds because

$$\begin{aligned} &\mathbb{E}[V - \sigma_N^2] \\ &= \mathbb{E}[X_A^2] \Delta \mathbb{E}[G] + 2\mathbb{E}[X_A] \Delta \mathbb{E}[Z_1] + \mathbb{E}[Z_0] - \sigma_N^2 \\ &= P\Delta \mathbb{E}[G] \geq 0. \end{aligned} \quad (69)$$

The monotonicity of the logarithmic function and (63) yield

$$\begin{aligned} \mathbb{E}[-\log(q_V(V))] &\geq \mathbb{E}\left[-\log\left(e^{P_{\min}/\lambda} f_V(V)\right)\right] \\ &\geq \log \Delta + \log \lambda - \frac{P_{\min}}{\lambda} \end{aligned} \quad (70)$$

where the last inequality follows from (68). It follows from (46), (60) and (70) that

$$\begin{aligned} I(X_A; V) &\geq \log \lambda - \frac{P_{\min}}{\lambda} - \frac{1}{2} \log(4\pi\sigma_N^2) - \frac{1}{2} \mathbb{E}[\log(X_A^2)] \\ &\quad - \frac{P}{4\sigma_N^2} \mathbb{E}[(G-1)^2] - \frac{1}{2} - \frac{\sigma_N^2}{4\Delta} \mathbb{E}\left[\frac{1}{X_A^2}\right]. \end{aligned} \quad (71)$$

If $P_{\min} = P/2$, then $\lambda = P - P_{\min} = P/2$ and we have

$$\mathbb{E}\left[\frac{1}{X_P}\right] \leq \frac{1}{P_{\min}} = \frac{2}{P} \quad (72)$$

and

$$\begin{aligned} \mathbb{E}[\log(X_P)] &= \int_\lambda^\infty \frac{1}{\lambda} e^{-(x-\lambda)/\lambda} \log(x) dx \\ &\stackrel{(a)}{=} \log \lambda + \int_1^\infty e^{-(u-1)} \log(u) du \\ &\stackrel{(b)}{\leq} \log \lambda + 1 \end{aligned} \quad (73)$$

where (a) follows by the change of variables $u = x/\lambda$, and (b) holds because $\log(u) \leq u - 1$ for all $u > 0$. Substituting into (71), we obtain

$$\begin{aligned} I(X_A; V) - \frac{1}{2} \log \text{SNR} &\geq -2 - \frac{1}{2} \log(8\pi) - \frac{1}{2\text{SNR}\Delta} \\ &\quad - \frac{1}{4} \text{SNR} \mathbb{E}[(G-1)^2]. \end{aligned} \quad (74)$$

By combining (35), (38), (40) and (74), we have

$$\begin{aligned} I(X_A; \mathbf{Y}) - \frac{1}{2} \log \text{SNR} &\geq -2 - \frac{1}{2} \log(8\pi) - \frac{1}{2\text{SNR}\Delta} \\ &\quad - \frac{1}{4} \text{SNR} \mathbb{E}[(G-1)^2]. \end{aligned} \quad (75)$$

Suppose L grows with SNR such that

$$L = \left\lceil \beta \sqrt{\text{SNR}} \right\rceil. \quad (76)$$

Since $\Delta = 1/L$, then we have

$$\lim_{\text{SNR} \rightarrow \infty} \text{SNR}\Delta = \infty \quad \text{and} \quad \lim_{\text{SNR} \rightarrow \infty} \text{SNR}\Delta^2 = \frac{1}{\beta^2} \quad (77)$$

which implies

$$\lim_{\text{SNR} \rightarrow \infty} \left[I(X_A; \mathbf{Y}) - \frac{1}{2} \log \text{SNR} \right] \geq -2 - \frac{1}{2} \log(8\pi) - \frac{\pi^2}{36} \quad (78)$$

because

$$\begin{aligned} &\lim_{\text{SNR} \rightarrow \infty} \text{SNR} \mathbb{E}[(G-1)^2] \\ &= \lim_{\text{SNR} \rightarrow \infty} \text{SNR}\Delta^2 \cdot \lim_{\Delta \rightarrow 0} \frac{\mathbb{E}[(G-1)^2]}{\Delta^2} \\ &= \frac{1}{\beta^2} \cdot \frac{(\pi\beta)^2}{9} = \frac{\pi^2}{9}. \end{aligned} \quad (79)$$

This can be shown by writing

$$\mathbb{E}[(G-1)^2] = \mathbb{E}[(G - \mathbb{E}[G])^2] + (\mathbb{E}[G] - 1)^2 \quad (80)$$

then computing

$$\lim_{\Delta \rightarrow 0} \frac{\mathbb{E}[(G-1)^2]}{\Delta^2} = \lim_{\Delta \rightarrow 0} \frac{\text{Var}(G)}{\Delta^2} + \lim_{\Delta \rightarrow 0} \frac{(\mathbb{E}[G] - 1)^2}{\Delta^2} = \frac{(\pi\beta)^2}{9}. \quad (81)$$

by using (see (220) and (221) in Appendix A.4)

$$\lim_{\Delta \rightarrow 0} \frac{\text{Var}(G)}{\Delta^2} = 0 \quad \text{and} \quad \lim_{\Delta \rightarrow 0} \frac{(\mathbb{E}[G] - 1)^2}{\Delta^2} = \frac{(\pi\beta)^2}{9}.$$

The main result of this section is summarized in following theorem.

Theorem 1: If $L = \lceil \beta \sqrt{\text{SNR}} \rceil$ and the input X_A^n is i.i.d. such that $(|X_k|^2 - P/2)$ is exponentially distributed with mean $P/2$, i.e., $|X_k|^2$ is distributed according to p_{X_P} where

$$p_{X_P}(|x|^2) = \begin{cases} \frac{2}{P} \exp\left(1 - \frac{2|x|^2}{P}\right), & |x|^2 \geq P/2 \\ 0, & \text{otherwise} \end{cases} \quad (82)$$

then

$$\lim_{\text{SNR} \rightarrow \infty} I(X_A; \mathbf{Y}) - \frac{1}{2} \log \text{SNR} \geq -2 - \frac{1}{2} \log(8\pi) - \frac{\pi^2}{36}. \quad (83)$$

The lower bound is achieved by the double-filtering¹ receiver structure shown in Fig. 5.

As a result, the capacity pre-log satisfies

$$\lim_{\text{SNR} \rightarrow \infty} \frac{C(\text{SNR})}{\log \text{SNR}} \geq \frac{1}{2} \quad (84)$$

which follows from Theorem 1 and $C(\text{SNR}) \geq I(X; \mathbf{Y}) \geq I(X_A; \mathbf{Y})$. The capacity thus grows logarithmically at high SNR with a pre-log factor of at least 1/2.

Remarks

- There is a wide literature on the design of receivers for the channel model (1) with discrete-time Wiener phase noise, e.g., see [32], [33], [34], [14] and references therein. One may want to use these designs, which raises the following question: “when is it justified to approximate the non-coherent fading model (3) with the discrete-time phase noise model (1)?” Our result suggests that this approximation may be justified when the phase variation is small over one symbol interval (i.e., when the phase noise linewidth is small compared to the symbol rate) and also the SNR is low to moderate. Note that the SNR at which the high-SNR asymptotics start to manifest themselves depends on the application.
- The authors of [21] treated on-off keying transmission in the presence of Wiener phase noise by using a double-filtering receiver, which is composed of an intermediate frequency (IF) filter, followed by an envelope detector (square-law device) and then a post-detection filter. They showed that by optimizing the IF receiver bandwidth the double-filtering receiver outperforms the single-filtering (matched filter) receiver. Furthermore, they showed via computer simulation that the optimum IF bandwidth increases with the SNR. This is similar to our result in the sense that we require the number of samples per symbol to increase with the SNR in order to achieve a rate that grows logarithmically with the SNR.
- Dallal and Shamai [35] derived an upper bound on the error probability of (a variant of) the double filtering receiver for systems employing noncoherent demodulation, such as frequency shift keying (FSK), on-off keying (OOK) and pulse-position modulation (PPM). Relevant analysis can be found in [36], [37] and references therein. The analysis in such papers typically involves moments of filtered Wiener phase noise. Dallal and Shamai [38]

examined coding schemes that do not use double filtering receivers. More specifically, the suggested coding scheme in [38] is a concatenated code with differential modulation and differential detection of binary phase-shift keying (BPSK) signals. They studied binary convolutional codes with a rate-1/L repetition code as the inner code. They also studied dual convolutional codes and Reed-Solomon block codes as outer codes with either simplex (maximal length) or bi-orthogonal (first-order Reed-Muller and Hadamard codes) as inner codes.

- One can achieve a pre-log of 1/2 with L less than $\lceil \beta \sqrt{\text{SNR}} \rceil$. For instance, suppose we use the auxiliary channel (48) with the same \tilde{Z}_1 and \tilde{Z}_0 defined in (50) and (51), respectively, but set $\tilde{G} = \mathbb{E}[G]$ rather than $\tilde{G} = 1$ as in (49). By using steps similar to the steps used to derive (75), we obtain

$$I(X_A; \mathbf{Y}) - \frac{1}{2} \log \text{SNR} \geq -2 - \frac{1}{2} \log(8\pi) - \frac{1}{2\text{SNR}\Delta} - \frac{1}{4} \text{SNR} \mathbb{E}[(G - \mathbb{E}[G])^2]. \quad (85)$$

Now choose

$$L = \left\lceil \sqrt[3]{\beta^2 \text{SNR}} \right\rceil. \quad (86)$$

Since $\Delta = 1/L$, it follows that

$$\lim_{\text{SNR} \rightarrow \infty} \text{SNR}\Delta = \infty \text{ and } \lim_{\text{SNR} \rightarrow \infty} \text{SNR}\Delta^3 = \frac{1}{\beta^2}. \quad (87)$$

Moreover, we have (see Appendix A.3)

$$\begin{aligned} \lim_{\text{SNR} \rightarrow \infty} \text{SNR} \text{Var}(G) &= \lim_{\text{SNR} \rightarrow \infty} \text{SNR}\Delta^3 \cdot \lim_{\Delta \rightarrow 0} \frac{\text{Var}(G)}{\Delta^3} \\ &= \frac{1}{\beta^2} \cdot \frac{4(\pi\beta)^2}{45} = \frac{4\pi^2}{45}. \end{aligned} \quad (88)$$

Hence, we have

$$\lim_{\text{SNR} \rightarrow \infty} I(X_A; \mathbf{Y}) - \frac{1}{2} \log \text{SNR} \geq -2 - \frac{1}{2} \log(8\pi) - \frac{\pi^2}{45}. \quad (89)$$

This means that a pre-log of 1/2 is achieved if the oversampling factor L grows with the cubic root of SNR.

V. RATE COMPUTATION AT FINITE SNR

In this section, we develop algorithms to compute the information rate numerically. We change the notation in this section as follows: we denote the input *symbols* with a subscript “symb”, i.e., the input codeword is $(X_{\text{symb},1}, X_{\text{symb},2}, \dots, X_{\text{symb},b})$ and we use X_k to denote the k th input *sample* which is defined by

$$X_k = X_{\text{symb}, \lceil k/L \rceil} g((k \bmod L)\Delta). \quad (90)$$

We write (18) as

$$Y_k = X_{\text{symb}, \lceil k/L \rceil} \Delta e^{j\Theta_k} F_k + N_k. \quad (91)$$

The information rate $I(X; Y)$ is defined as

$$I(X; Y) \equiv \lim_{b \rightarrow \infty} \frac{1}{b} I(X_{\text{symb}}^b; \mathbf{Y}^b) = \lim_{b \rightarrow \infty} \frac{1}{b} I(X^n; Y^n) \quad (92)$$

¹We borrow the term “double-filtering” from [20].

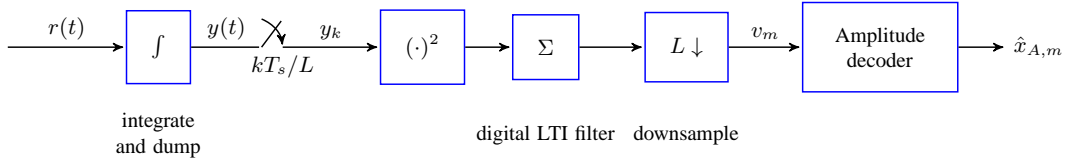


Fig. 5. Double filtering receiver.

where the last equality follows from the definitions (90) and (31). One difficulty in evaluating (92) is that the joint distribution of $\{F_k\}$ and $\{W_k\}$ is not available in closed form. Even the distribution of F_k is not available in closed form (there is an approximation for small linewidth, see (16) in [21]). However, we can numerically compute tight lower bounds on $I(X; Y)$ by using the auxiliary-channel technique described in (46) and (47). That is, we have

$$I(X; Y) \geq \underline{I}(X; Y) = \mathbb{E} \left[\log \left(\frac{q_{Y|X}(Y|X)}{q_Y(Y)} \right) \right] \quad (93)$$

where $q_{Y|X}(\cdot|\cdot)$ is an arbitrary auxiliary channel and

$$q_Y(y) = \sum_{\tilde{x}} p_X(\tilde{x}) q_{Y|X}(y|\tilde{x}) \quad (94)$$

where p_X is the *true* distribution of X . The distribution $q_Y(\cdot)$ is the output distribution obtained by connecting the true input source to the auxiliary channel. Using this result, we can compute a lower bound on $I(X; Y)$ by using the following algorithm [11]:

- 1) Sample a long sequence (x^n, y^n) according to the *true* joint distribution of X^n and Y^n ;
- 2) Compute $q_{Y^n|X^n}(y^n|x^n)$ and

$$q_{Y^n}(y^n) = \sum_{\tilde{x}^n} p_{X^n}(\tilde{x}^n) q_{Y^n|X^n}(y^n|\tilde{x}^n) \quad (95)$$

where p_{X^n} is the true distribution of X^n ;

- 3) Estimate $\underline{I}(X; Y)$ using

$$\underline{I}(X; Y) \approx \frac{1}{b} \log \left(\frac{q_{Y^n|X^n}(y^n|x^n)}{q_{Y^n}(y^n)} \right). \quad (96)$$

Auxiliary Channel I: Consider the auxiliary channel

$$\Psi_k = X_k \Delta e^{j\Theta_k} + N_k \quad (97)$$

where $\{\Theta_k\}$ and $\{N_k\}$ are defined in Sec. III-C and X_k is defined by (90). The channel output Ψ is the same as Y in (91) *except* that F_k is replaced by 1 or more generally with $g((k \bmod L)\Delta)$. The channel is described by the conditional distribution

$$p_{\Psi^n|X^n}(y^n|x^n) = \int_{\theta^n} p_{\Theta^n, \Psi^n|X^n}(\theta^n, y^n|x^n) d\theta^n \quad (98)$$

where

$$\begin{aligned} & p_{\Theta^n, \Psi^n|X^n}(\theta^n, y^n|x^n) \\ &= \prod_{k=1}^n p_{\Theta_k|\Theta_{k-1}}(\theta_k|\theta_{k-1}) p_{\Psi|X, \Theta}(y_k|x_k, \theta_k) \end{aligned} \quad (99)$$

with

$$p_{\Theta_k|\Theta_{k-1}}(\theta|\tilde{\theta}) = \begin{cases} p_W(\theta - \tilde{\theta}; \sigma_W^2), & k \geq 2 \\ 1/(2\pi), & k = 1 \end{cases} \quad (100)$$

and

$$p_{\Psi|X, \Theta}(y|x, \theta) = \frac{1}{\pi \sigma_N^2 \Delta} \exp \left(-\frac{|y - x e^{j\theta}|^2}{\sigma_N^2 \Delta} \right). \quad (101)$$

The channel $p_{\Psi^n|X^n}$ has continuous states θ^n , which makes step 2 of the algorithm computationally infeasible.

Auxiliary Channel II: We use the following auxiliary channel for the numerical simulations:

$$\Upsilon_k = X_k \Delta e^{jS_k} + N_k \quad (102)$$

which has the conditional probability

$$p_{\Upsilon^n|X^n}(y^n|x^n) = \sum_{s^n \in \mathcal{S}^n} p_{S^n, \Upsilon^n|X^n}(s^n, y^n|x^n) \quad (103)$$

where \mathcal{S} is a *finite* set and

$$\begin{aligned} & p_{S^n, \Upsilon^n|X^n}(s^n, y^n|x^n) \\ &= \prod_{k=1}^n p_{S_k|S_{k-1}}(s_k|s_{k-1}) p_{\Psi|X, \Theta}(y_k|x_k, s_k) \end{aligned} \quad (104)$$

where

$$p_{S_k|S_{k-1}}(s|\tilde{s}) = \begin{cases} Q(s|\tilde{s}), & k \geq 2 \\ 1/|S|, & k = 1. \end{cases} \quad (105)$$

Next, we describe our choice of \mathcal{S} and $Q(\cdot|\cdot)$. We partition $[-\pi, \pi)$ into S intervals with equal lengths and pick the mid points of these intervals to be the elements of \mathcal{S} , i.e., we have

$$\mathcal{S} = \{\hat{s}_i : i = 1, \dots, S\} \text{ where } \hat{s}_i = i \frac{2\pi}{S} - \frac{\pi}{S} - \pi. \quad (106)$$

The state transition probability $Q(\cdot|\cdot)$ is chosen similar to [10] and [12]:

$$Q(s|\tilde{s}) = \frac{2\pi}{S} \int_{(\phi, \tilde{\phi}) \in \mathcal{R}(s) \times \mathcal{R}(\tilde{s})} p_W(\phi - \tilde{\phi}; \sigma_W^2) d\phi d\tilde{\phi} \quad (107)$$

where $\mathcal{R}(s) = [s - \pi/S, s + \pi/S)$, i.e., $\mathcal{R}(s)$ is the interval whose midpoint is s . The larger S and L are, the better the auxiliary channel (102) approximates the actual channel (91). We remark that the auxiliary channel gives a *valid* lower bound on $I(X; Y)$ even for small S and L .

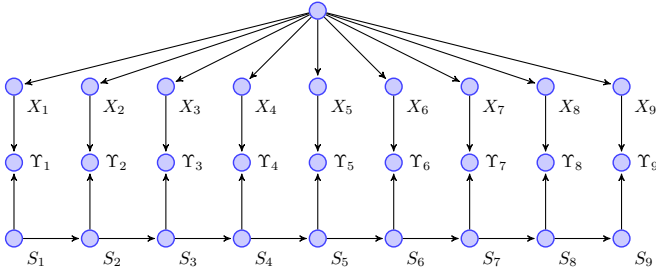


Fig. 6. Bayesian network for X^n, S^n, Y^n for $n = 9$.

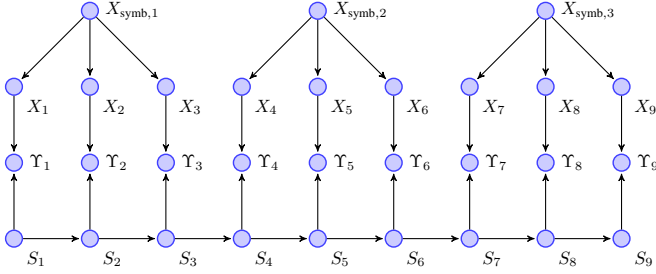


Fig. 7. Bayesian network for X^n, S^n, Y^n for $n = 9$ and $L = 3$.

A. Computing The Conditional Probability

Suppose the input X^n has the distribution p_{X^n} . A Bayesian network for X^n, S^n, Y^n is shown in Fig. 6. The probability $p_{Y^n|X^n}(y^n|x^n)$ can be computed using

$$p_{Y^n|X^n}(y^n|x^n) = \sum_{s \in \mathcal{S}} \rho_n(s) \quad (108)$$

where we recursively compute

$$\begin{aligned} \rho_k(s) &\equiv p_{S_k, Y^k|X^n}(s, y^k|x^n) \quad (109) \\ &\stackrel{(a)}{=} \sum_{\tilde{s} \in \mathcal{S}} p_{S_{k-1}, S_k, Y^k|X^n}(\tilde{s}, s, y^k|x^n) \\ &\stackrel{(b)}{=} \sum_{\tilde{s} \in \mathcal{S}} \rho_{k-1}(\tilde{s}) p_{S_k, Y_k|S_{k-1}, Y^{k-1}, X^n}(s, y_k|\tilde{s}, y^{k-1}, x^n) \\ &= \sum_{\tilde{s} \in \mathcal{S}} \rho_{k-1}(\tilde{s}) Q(s|\tilde{s}) p_{Y|X, \Theta}(y_k|x_k, s) \quad (110) \end{aligned}$$

with the initial value $\rho_0(s) = 1/|\mathcal{S}|$. Step (a) is a marginalization, (b) follows from Bayes' rule and the definition of ρ_k in (109), while (110) follows from the structure of Fig. 6. We remark that (110) is the same as with independent X_1, \dots, X_n , e.g., see equation (9) in [39, Sec. IV].

B. Computing The Marginal Probability

Define $\mathbf{X}_m \equiv (X_{(m-1)L+1}, X_{(m-1)L+2}, \dots, X_{(m-1)L+L})$. Suppose the input symbols are i.i.d. and $X_m \in \mathcal{X}$ where \mathcal{X} is a finite set. Therefore, p_{X^n} has the form

$$p_{X^n}(x^n) = \prod_{m=1}^b p_{\mathbf{X}}(\mathbf{x}_m). \quad (111)$$

A Bayesian network for X^n, S^n, Y^n is shown in Fig. 7. The probability $p_{Y^n}(y^n)$ can be computed using

$$p_{Y^n}(y^n) = \sum_{s \in \mathcal{S}} \psi_b(s) \quad (112)$$

where $\psi_m(s) \equiv p_{S_{mL}, Y^m}(s, \mathbf{y}^m)$ which can be computed using the recursion:

$$\begin{aligned} \psi_m(s) &\quad (113) \\ &= \sum_{\tilde{\mathbf{x}} \in \mathcal{X}_L} p_{\mathbf{X}}(\tilde{\mathbf{x}}) \sum_{\tilde{s} \in \mathcal{S}} \psi_{m-1}(\tilde{s}) p_{S_{mL}, Y^m|S_{(m-1)L}, \mathbf{X}_m}(s, \mathbf{y}_m|\tilde{s}, \tilde{\mathbf{x}}) \end{aligned}$$

with the initial value $\psi_0(s) = 1/|\mathcal{S}|$. The set \mathcal{X}_L is

$$\mathcal{X}_L = \{x \cdot (g(\Delta), g(2\Delta), \dots, g(L\Delta)) : x \in \mathcal{X}\}. \quad (114)$$

We remark that $|\mathcal{X}_L| = |\mathcal{X}|$ and not $|\mathcal{X}|^L$. Next, we define

$$\chi_{m,L}(s, \tilde{s}, \tilde{\mathbf{x}}) = p_{S_{mL}, Y^m|S_{(m-1)L}, \mathbf{X}_m}(s, \mathbf{y}_m|\tilde{s}, \tilde{\mathbf{x}}) \quad (115)$$

for $s, \tilde{s} \in \mathcal{S}$ and $\tilde{\mathbf{x}} \in \mathcal{X}_L$. Computing $\chi_{m,L}(s, \tilde{s}, \tilde{\mathbf{x}})$ is similar to computing ρ_n (see (110)). Intuitively, this is because a block of L samples in Fig. 7 has a structure similar to Fig. 6. More precisely, $\chi_{m,L}(s, \tilde{s}, \tilde{\mathbf{x}})$ can be computed recursively by using

$$\begin{aligned} \chi_{m,\ell}(s, \tilde{s}, \tilde{\mathbf{x}}) &\quad (116) \\ &= \sum_{\varsigma \in \mathcal{S}} \chi_{m,\ell-1}(\varsigma, \tilde{s}, \tilde{\mathbf{x}}) Q(s|\varsigma) p_{Y|X, \Theta}(y_{(m-1)L+\ell}|\tilde{x}_\ell, s) \end{aligned}$$

with the initial value

$$\chi_{m,0}(s, \tilde{s}, \tilde{\mathbf{x}}) = \begin{cases} 1, & s = \tilde{s} \\ 0, & \text{otherwise.} \end{cases} \quad (117)$$

Therefore, computing $p_{Y^n}(y^n)$ involves two levels of recursion: 1) recursion over the symbols as described by (113) and 2) recursion over the samples within a symbol as described by (116).

VI. NUMERICAL SIMULATIONS

We use two pulses with a symbol-interval time support:

- A unit-energy square pulse

$$g_1(t) = \frac{1}{\sqrt{T_s}} \text{rect}\left(\frac{t}{T_s}\right) \quad (118)$$

where

$$\text{rect}(t) \equiv \begin{cases} 1, & |t| \leq 1/2, \\ 0, & \text{otherwise.} \end{cases} \quad (119)$$

- A unit-energy cosine-squared pulse

$$g_2(t) = \frac{1}{\sqrt{T_s/2}} \cos^2\left(\frac{\pi t}{T_s}\right) \text{rect}\left(\frac{t}{T_s}\right). \quad (120)$$

The first step of the algorithm is to sample a long sequence according to the true joint distribution of X^n and Y^n . To generate samples according to the original channel (91), we must accurately represent digitally the continuous-time waveform (4). We use a simulation oversampling rate $L_{\text{sim}} = 1024$ samples/symbol. After the filter (17), the receiver has L samples/symbol distributed according to (91). Next, to choose a proper sequence length, we follow the approach suggested in [11]: for a candidate length, run the algorithm about 10 times (each with a new random seed) and check whether all estimates of the information rate agree up to the desired accuracy. We used $b = 10^4$ unless otherwise stated.

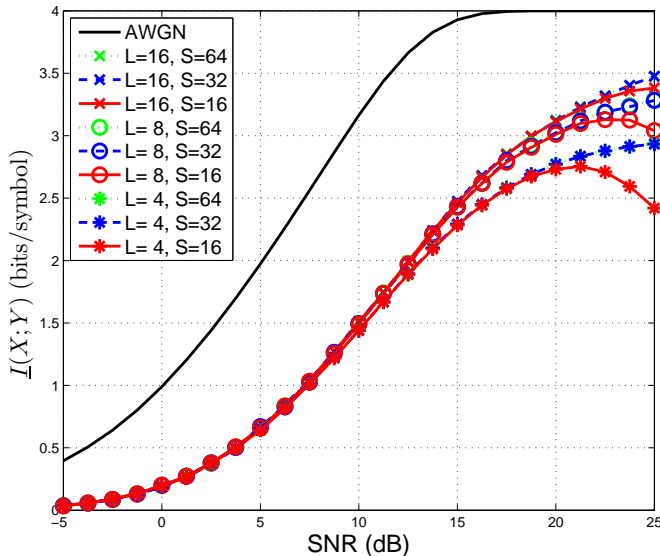


Fig. 8. Lower bounds on rates for 16-QAM, square transmit-pulse and multi-sample receiver at $f_{\text{HWHM}}T_s = 0.125$.

For efficient implementation of (110), $p_{\Psi|X,\Theta}(\cdot|\cdot, \cdot)$ can be factored out of the summation to yield:

$$\rho_k(s) = p_{\Psi|X,\Theta}(y_k|x_k, s) \overbrace{\sum_{\tilde{s} \in S} \rho_{k-1}(\tilde{s}) Q(s|\tilde{s})}^{\rho'_k(s)} \quad (121)$$

Moreover, since $Q(\cdot|\cdot)$ can be represented by a circulant matrix due to symmetry, $\rho'_k(\cdot)$ can be computed efficiently using the Fast Fourier Transform (FFT). Similarly, the computation of (116) can be done efficiently by factoring out $p_{\Psi|X,\Theta}(\cdot|\cdot, \cdot)$ and by using the FFT.

A. Excessively Large Linewidth

Suppose $f_{\text{HWHM}}T_s = 0.125$ and the input symbols are independently and uniformly distributed (i.u.d.) 16-QAM. Fig. 8 shows an estimate of $\underline{I}(X; Y)$ for a square transmit-pulse, i.e., $g(t) = g_1(t - T_s/2)$ and an L -sample receiver with $L = 4, 8, 16$ and $S = 16, 32, 64$. The curves with $S = 64$ are indistinguishable from the curves with $S = 32$ over the entire SNR range for all values of L , and hence $S = 32$ is adequate up to 25 dB. Even $S = 16$ is adequate up to 20 dB. The important trend in Fig. 8 is that higher oversampling rate L is needed at high SNR to extract all the information from the received signal. For example, $L = 4$ suffices up to $\text{SNR} \sim 10$ dB, $L = 8$ suffices up to $\text{SNR} \sim 15$ dB but $L \geq 16$ is needed beyond that. It was pointed out in [11] that the lower bounds can be interpreted as the information rates achieved by mismatched decoding. For example, $\underline{I}(X; Y)$ for $L = 8$ and $S \geq 32$ in Fig. 8 is essentially the information rate achieved by a multi-sample (8-sample) receiver that uses maximum-likelihood decoding for the simplified channel (97) when it is operated in the original channel (91).

Fig. 9 shows an estimate of $\underline{I}(X; Y)$ for a cosine-squared transmit-pulse, i.e., $g(t) = g_2(t - T_s/2)$ and an L -sample receiver at $L = 4, 8, 16$ and $S = 16, 32, 64$. We find that

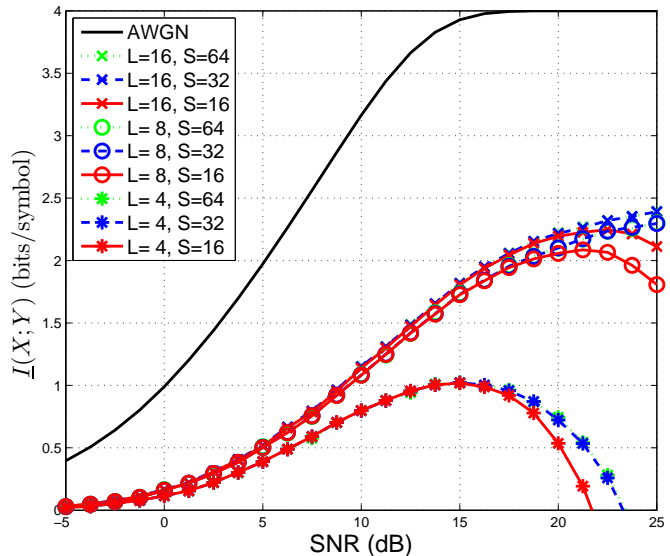


Fig. 9. Lower bounds on rates for 16-QAM, cosine-squared transmit-pulse and multi-sample receiver at $f_{\text{HWHM}}T_s = 0.125$.

$S = 32$ suffices up to ~ 25 dB. We see in Fig. 9 the same trend in Fig. 8: higher L is needed at higher SNR. Comparing Fig. 8 with Fig. 9 indicates that the square pulse is better than the cosine-squared pulse for the same oversampling rate L . It might seem strange that the cosine-squared pulse curves are substantially lower than the square pulse curves despite taking into account the pulse shape in the auxiliary channel model, see (102) and (90). One obtains insight on this effect with the following Gedankenexperiment. Suppose we use a pulse that is narrow and peaky in time. Then an integrate-and-dump receiver with oversampling puts out essentially only one useful sample per symbol. One may as well, therefore, use only one sample per symbol.

B. Large Linewidth

As the linewidth decreases, the benefit of oversampling at the receiver becomes apparent only at higher SNR. For example, for $f_{\text{HWHM}}T_s = 0.0125$ and i.u.d. 16-PSK input, Fig. 10 shows an estimate of $\underline{I}(X; Y)$ for a square transmit-pulse and an L -sample receiver at $L = 1, 2, 4, 8, 16$ and $S = 64$. We see that $L = 4$ suffices up to $\text{SNR} \sim 19$ dB, $L = 8$ suffices up to $\text{SNR} \sim 24$ dB and only beyond that $L \geq 16$ is necessary.

We conclude from Fig. 8–10 that the required L depends on 1) the linewidth f_{FWHM} of the phase noise; 2) the pulse $g(t)$; and 3) the SNR.

C. Comparison With Other Models

We compare the discrete-time model of the multi-sample receiver with other discrete-time models. The simulation parameters for our model (GK) are $b = 10^4$, $L = 16$ (with $L_{\text{sim}} = 1024$) and $S = 64$ for 16-QAM ($S = 128$ was too computationally intensive) and $S = 128$ for QPSK.

In Fig. 11, we show curves for the Baud-rate model used in [14] and [9]–[13]. The model is (1) where the phase noise is a Wiener process whose noise increments have variance γ^2 . We

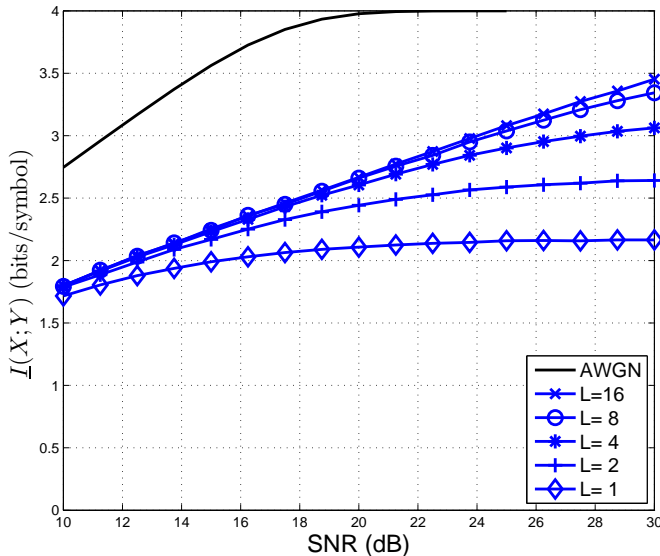


Fig. 10. Lower bounds on rates for 16-PSK, square transmit-pulse and multi-sample receiver at $f_{\text{HWHM}}T_s = 0.0125$.

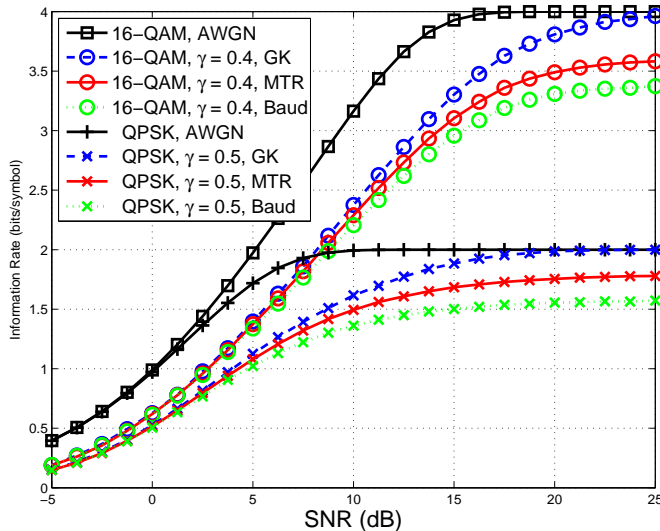


Fig. 11. Comparison of information rates for different models.

set $\gamma^2 = 2\pi\beta T_s$. The simulation parameters for the Baud-rate model are $b = 10^5$ and $S = 128$.

We also show curves for the Martalò-Tripodi-Raheli (MTR) model [39] in Fig. 11. For the sake of comparison, we adapt the model in [39] from a square-root raised-cosine pulse to a square pulse and write the “matched” filter output $\{V_m\}$ as

$$V_m = \sum_{\ell=1}^L \Psi_{(m-1)L+\ell} \quad (122)$$

where $m = 1, \dots, b$ and Ψ_k is defined in (97). The auxiliary channel is

$$Y_m = X_{\text{symp},m} e^{j\Theta_m} + Z_m, \quad m \geq 1 \quad (123)$$

where the process $\{Z_m\}$ is an i.i.d. circularly-symmetric complex Gaussian process with mean 0 and $\mathbb{E}[|Z_m|^2] = \sigma_N^2 T_s$ while the process $\{\Theta_m\}$ is a first-order Markov process

(not a Wiener process) with a time-invariant transition probability, i.e., for $k \geq 2$ and all $\theta_k, \theta_{k-1} \in [-\pi, \pi)$, we have $p_{\Theta_k|\Theta_{k-1}}(\theta_k|\theta_{k-1}) = p_{\Theta_2|\Theta_1}(\theta_k|\theta_{k-1})$. Furthermore, the phase space is quantized to a finite number S of states and the transition probabilities are estimated by means of simulation. The probabilities are then used to compute a lower bound on the information rate. The simulation parameters for the MTR model are $b = 10^5$, $L = 16$ and $S = 128$.

We see that the Baud-rate and MTR models saturate at a rate well below the rate achieved by the multi-sample receiver. Moreover, the multi-sample receiver achieves the full 4 bits/symbol and 2 bits/symbol of 16-QAM and QPSK, respectively, at high SNR.

VII. HIGH SNR REVISITED

In this section, we focus on the contribution of phase modulation to capacity. However, solving the problem for the model given by (18) seems difficult. The model we adopt in this section does not include the effect of filtering modeled by $\{F_k\}$. More specifically, the k th output of the simplified approximate model is

$$Y_k = X_{[k/L]} \Delta e^{j\Theta_k} + N_k \quad (124)$$

where X_k is k th input symbol and $\{\Theta_k\}$ and $\{N_k\}$ are the same processes defined in Sec. III-C.

First, we show in Sec. VII-A that phase modulation achieves an information rate with a pre-log of $1/2$ in an AWGN channel. Even though this result is already known (e.g., see [40], [41] or [17]), the technique used in the proof is useful, as we will see. We show in Sec. VII-B that the contribution of phase modulation to the pre-log is at least $1/4$ for the approximate model in (124).

A. Phase Modulation in AWGN Channels

We develop a lower bound on the information rate achieved by phase modulation on an AWGN channel which shows that phase modulation achieves a pre-log of $1/2$ at high SNR. Let R be a fixed positive real number. Consider the channel whose output Y is

$$Y = R e^{j\phi_X} + Z \quad (125)$$

where $\phi_X \in [-\pi, \pi)$ is the input and Z is a circularly-symmetric complex Gaussian random variable with mean 0 and variance 1. Define $\Phi_Y \equiv \angle Y$. The conditional probability $p_{\Phi_Y|\Phi_X}$ is given by [42]

$$p_{\Phi_Y|\Phi_X}(\phi_y|\phi_x) = p_{\Phi}(\phi_y - \phi_x) \quad (126)$$

with

$$p_{\Phi}(\phi) = \frac{1}{2\pi} e^{-R^2} + \frac{1}{\sqrt{4\pi}} R \cos(\phi) e^{-R^2 \sin^2 \phi} \text{erfc}(-R \cos \phi) \quad (127)$$

where $\text{erfc}(\cdot)$ is the complementary error function

$$\text{erfc}(z) \equiv \frac{2}{\sqrt{\pi}} \int_z^{\infty} e^{-t^2} dt. \quad (128)$$

Lemma 2: Fix $R > 0$. For the channel Y described by (125), we have

$$\mathbb{E}[\cos(\Phi_Y - \Phi_X)] = \mathbb{E}[\cos(\Phi)] \geq 1 - \frac{1}{R^2} \quad (129)$$

$$\mathbb{E}[\sin(\Phi_Y - \Phi_X)] = \mathbb{E}[\sin(\Phi)] = 0 \quad (130)$$

where Φ is a random variable with the probability density function p_Φ given by (127).

Proof: From symmetry (see Lemma 12), we have

$$\mathbb{E}[\cos(\Phi_Y - \Phi_X)] = \mathbb{E}[\cos(\Phi)] \quad (131)$$

and

$$\begin{aligned} \mathbb{E}[\cos(\Phi)] &\equiv \int_{-\pi}^{\pi} \cos(\phi) p_\Phi(\phi) d\phi \\ &\stackrel{(a)}{=} 2 \int_0^{\pi} \cos(\phi) p_\Phi(\phi) d\phi \\ &\stackrel{(b)}{=} \int_0^{\pi} \cos(\phi) \left[\frac{1}{\sqrt{\pi}} R \cos(\phi) e^{-R^2 \sin^2 \phi} \operatorname{erfc}(-R \cos \phi) \right] d\phi \\ &\stackrel{(c)}{\geq} \int_0^{\pi/2} \frac{R}{\sqrt{\pi}} \cos^2(\phi) e^{-R^2 \sin^2 \phi} \operatorname{erfc}(-R \cos \phi) d\phi \\ &\stackrel{(d)}{\geq} \int_0^{\pi/2} \frac{R}{\sqrt{\pi}} \cos^2(\phi) e^{-R^2 \sin^2 \phi} (2 - e^{-R^2 \cos^2 \phi}) d\phi \\ &= \int_0^{\pi/2} \frac{2R}{\sqrt{\pi}} \cos^2(\phi) e^{-R^2 \sin^2 \phi} d\phi - \frac{R}{\sqrt{\pi}} e^{-R^2} \int_0^{\pi/2} \cos^2 \phi d\phi \\ &\stackrel{(e)}{=} \int_0^{\pi/2} \frac{2R}{\sqrt{\pi}} \cos^2(\phi) e^{-R^2 \sin^2 \phi} d\phi - \frac{\sqrt{\pi}}{4} R e^{-R^2} \quad (132) \end{aligned}$$

where (a) follows because both $p_\Phi(\cdot)$ and $\cos(\phi)$ are even functions, (b) follows from (127) and $\int_0^\pi \cos \phi d\phi = 0$, (c) follows because the integrand is non-negative over the interval $\phi \in (\pi/2, \pi]$, (d) holds because $\operatorname{erfc}(-R \cos \phi) \geq 2 - e^{-R^2 \cos^2 \phi}$ (see Lemma 13) and $\cos^2(\phi) e^{-R^2 \sin^2 \phi} \geq 0$ and finally (e) follows by direct integration.

We bound the integral in (132) as follows

$$\begin{aligned} &\int_0^{\pi/2} \frac{2R}{\sqrt{\pi}} \cos^2 \phi e^{-R^2 \sin^2 \phi} d\phi \\ &\stackrel{(a)}{\geq} \frac{2R}{\sqrt{\pi}} \int_0^{\pi/2} (1 - \phi^2) e^{-R^2 \phi^2} d\phi \\ &= \frac{2R}{\sqrt{\pi}} \int_0^{\pi/2} e^{-R^2 \phi^2} d\phi - \frac{2R}{\sqrt{\pi}} \int_0^{\pi/2} \phi^2 e^{-R^2 \phi^2} d\phi \\ &\stackrel{(b)}{=} \operatorname{erf}\left(\frac{\pi}{2} R\right) - \frac{1}{2R^2} \operatorname{erf}\left(\frac{\pi}{2} R\right) + \frac{1}{2\sqrt{\pi} R} e^{-\pi^2 R^2/4} \\ &\stackrel{(c)}{\geq} \operatorname{erf}\left(\frac{\pi}{2} R\right) - \frac{1}{2R^2} \quad (133) \end{aligned}$$

where $\operatorname{erf}(\cdot)$ is the error function defined as

$$\operatorname{erf}(z) \equiv \frac{2}{\sqrt{\pi}} \int_0^z e^{-t^2} dt. \quad (134)$$

Step (a) follows from $\cos^2 \phi e^{-R^2 \sin^2 \phi} \geq (1 - \phi^2) e^{-R^2 \phi^2}$ (see Lemma 15), (b) follows by using the definition of $\operatorname{erf}(\cdot)$ and [43, 3.321(5)]:

$$\int_0^b t^2 e^{-a^2 t^2} dt = \frac{1}{2a^3} \left[\frac{\sqrt{\pi}}{2} \operatorname{erf}(ab) - ab e^{-a^2 b^2} \right] \quad (135)$$

and (c) holds because $\operatorname{erf}(\cdot) \leq 1$ and the last term is non-negative. Substituting back in (132) yields

$$\mathbb{E}[\cos(\Phi)] \geq \operatorname{erf}\left(\frac{\pi}{2} R\right) - \frac{1}{2R^2} - \frac{\sqrt{\pi}}{4} R e^{-R^2} \quad (136)$$

$$\geq 1 - e^{-\pi^2 R^2/4} - \frac{1}{2R^2} - \frac{\sqrt{\pi}}{4} R e^{-R^2} \quad (137)$$

where the last inequality follows from the relations $\operatorname{erf}(\pi R/2) = 1 - \operatorname{erfc}(\pi R/2)$ and $\operatorname{erfc}(\pi R/2) \leq e^{-\pi^2 R^2/4}$ (see [44, eq(5)]). Therefore, we have

$$R^2 \mathbb{E}[\cos(\Phi)] \geq R^2 - \frac{4}{\pi^2 e} - \frac{1}{2} - \frac{\sqrt{\pi}}{4} \left(\frac{3}{2e}\right)^{3/2} \quad (138)$$

because $R^3 e^{-R^2} \leq (3/2e)^{3/2}$ and $R^2 e^{-\pi^2 R^2/4} \leq 4/\pi^2 e$ (see Lemma 16). We conclude that

$$\mathbb{E}[\cos(\Phi)] \geq 1 - \frac{0.83}{R^2} \geq 1 - \frac{1}{R^2}. \quad (139)$$

We remark that

$$\mathbb{E}[\sin(\Phi)] \equiv \int_{-\pi}^{\pi} \sin(\phi) p_\Phi(\phi) d\phi = 0 \quad (140)$$

because the integrand is odd. Therefore, it follows from the symmetry (see Lemma 12) and (140) that

$$\mathbb{E}[\sin(\Phi_Y - \Phi_X)] = 0. \quad (141)$$

Lemma 3: Fix $R > 0$. Let Y be the channel described by (125). If the channel input Φ_X is uniformly distributed over $[-\pi, \pi)$, then we have

$$I(\Phi_X; Y) \geq I(\Phi_X; \Phi_Y) \geq \frac{1}{2} \log R^2 - 1. \quad (142)$$

Proof: Define

$$q_{\Phi_Y|\Phi_X}(\phi_y|\phi_x) \equiv \frac{\exp(\alpha \cos(\phi_y - \phi_x))}{2\pi I_0(\alpha)} \quad (143)$$

where $I_0(\cdot)$ is the modified Bessel function of the first kind of order zero and $\alpha > 0$. This distribution is known as Tikhonov (or von Mises) distribution [45]. Define

$$q_{\Phi_Y}(\phi_y) \equiv \int_{-\pi}^{\pi} p_{\Phi_X}(\phi_x) q_{\Phi_Y|\Phi_X}(\phi_y|\phi_x) d\phi_x \quad (144)$$

$$= \frac{1}{2\pi}. \quad (145)$$

The mutual information between the input phase Φ_X and the output phase Φ_Y is

$$\begin{aligned} I(\Phi_X; \Phi_Y) &\stackrel{(a)}{\geq} \mathbb{E}[\log(q_{\Phi_Y|\Phi_X}(\Phi_Y|\Phi_X))] - \mathbb{E}[\log(q_{\Phi_Y}(\Phi_Y))] \\ &\stackrel{(b)}{=} \log(2\pi) - \log(2\pi I_0(\alpha)) + \alpha \mathbb{E}[\cos(\Phi_Y - \Phi_X)] \\ &= -\log(I_0(\alpha)) + \alpha \mathbb{E}[\cos(\Phi_Y - \Phi_X)] \\ &\stackrel{(c)}{\geq} \frac{1}{2} \log \alpha - \alpha + \alpha \mathbb{E}[\cos(\Phi_Y - \Phi_X)] \quad (146) \end{aligned}$$

where (a) follows from the auxiliary-channel lower bound theorem in [11, Sec. VI], (b) follows from (145) and (143) and (c) follows from [46, Lemma 2]

$$I_0(z) \leq \frac{\sqrt{\pi}}{2} \frac{e^z}{\sqrt{z}} \leq \frac{e^z}{\sqrt{z}}. \quad (147)$$

By combining (146) and (129), we have

$$I(\Phi_X; \Phi_Y) \geq \frac{1}{2} \log \alpha - \frac{\alpha}{R^2}. \quad (148)$$

Therefore, setting $\alpha = R^2$ yields

$$I(\Phi_X; \Phi_Y) \geq \frac{1}{2} \log R^2 - 1. \quad (149)$$

B. Phase Modulation in Phase Noise Channels

In this section, we study the contribution of the phase modulation to the capacity of the channel (124) at high SNR. We assume that $T_s = 1$ and $\sigma_N^2 = 1$ for simplicity. By using the chain rule, we have

$$\begin{aligned} I(\Phi_X^n; \mathbf{Y}^n | X_A^n) &= \sum_{k=1}^n I(\Phi_{X,k}; \mathbf{Y}^n | X_A^n, \Phi_X^{k-1}) \\ &\stackrel{(a)}{\geq} \sum_{k=2}^n I(\Phi_{X,k}; \mathbf{Y}^n | X_A^n, \Phi_X^{k-1}) \\ &\stackrel{(b)}{\geq} \sum_{k=2}^n I(\Phi_{X,k}; \tilde{Y}_k | X_A^n, \Phi_X^{k-1}) \end{aligned} \quad (150)$$

where \tilde{Y}_k is a deterministic function of $(\mathbf{Y}^n, X_A^n, \Phi_X^{k-1})$. Inequality (a) follows from the non-negativity of mutual information and (b) follows from the data processing inequality.

At high SNR, we use some intuition to choose a reasonable processing of $(\mathbf{Y}^n, X_A^n, \Phi_X^{k-1})$ for decoding $\Phi_{X,k}$:

- 1) Since only the past inputs X^{k-1} are available, the future outputs \mathbf{Y}_{k+1}^n are not very useful for estimating $\Theta_{(k-1)L}$.
- 2) Since $\{\Theta_k\}$ is a first-order Markov process, the most recent past input symbol X_{k-1} and the most recent output sample $Y_{(k-1)L}$ are the most useful for estimating $\Theta_{(k-1)L}$. A simple estimator is

$$\begin{aligned} e^{j\hat{\Theta}_{(k-1)L}} &\equiv \frac{Y_{(k-1)L}}{X_{k-1}\Delta} = e^{j\Theta_{(k-1)L}} + \frac{N_{(k-1)L}}{X_{k-1}\Delta} \\ &= e^{j\Theta_{(k-1)L}} \left(1 + \tilde{Z}_{k-1}^*\right) \end{aligned} \quad (151)$$

where

$$\tilde{Z}_k \equiv \frac{N_{kL}^* e^{-j\Theta_{kL}}}{X_k^* \Delta}. \quad (152)$$

- 3) Given the current input amplitude $|X_k|$ and the estimate of $\Theta_{(k-1)L}$, the first sample $Y_{(k-1)L+1}$ in \mathbf{Y}_k is the most useful for decoding $\Phi_{X,k}$ because the following samples become increasingly corrupted by the phase noise. We scale $Y_{(k-1)L+1}$ to normalize the variance of the additive noise and write

$$\frac{Y_{(k-1)L+1}}{\sqrt{\Delta}} = \left(|X_k| \sqrt{\Delta} e^{j\Phi_{X,k}} + \tilde{N}_k\right) e^{j\Theta_{(k-1)L+1}} \quad (153)$$

where

$$\tilde{N}_k \equiv \frac{N_{(k-1)L+1} e^{-j\Theta_{(k-1)L+1}}}{\sqrt{\Delta}}. \quad (154)$$

To summarize, we choose

$$\tilde{Y}_k = \frac{Y_{(k-1)L+1}}{\sqrt{\Delta}} \left(\frac{Y_{(k-1)L}}{X_{k-1}\Delta}\right)^*. \quad (155)$$

It follows from (155), (151) and (153) that

$$\tilde{Y}_k = \left(|X_k| \sqrt{\Delta} e^{j\Phi_{X,k}} + \tilde{N}_k\right) \left(1 + \tilde{Z}_{k-1}\right) e^{jW_{(k-1)L+1}} \quad (156)$$

- where \tilde{N}_k and \tilde{Z}_{k-1} are statistically independent and

$$\tilde{N}_k \sim \mathcal{N}_{\mathbb{C}}(0, 1) \quad (157)$$

$$\tilde{Z}_{k-1} \left\{ |X_{k-1}| = |x_{k-1}| \right\} \sim \mathcal{N}_{\mathbb{C}} \left(0, \frac{1}{|x_{k-1}|^2 \Delta} \right). \quad (158)$$

The notation (158) means that, conditioned on $\{|X_{k-1}| = |x_{k-1}|\}$, \tilde{Z}_{k-1} is a Gaussian random variable with mean 0 and variance $1/(|x_{k-1}|^2 \Delta)$. Moreover, $W_{(k-1)L+1}$ is statistically independent of \tilde{N}_k and \tilde{Z}_{k-1} . The choice of \tilde{Y}_k in (155) implies that

$$I(\Phi_{X,k}; \tilde{Y}_k | X_A^n, X^{k-1}) = I(\Phi_{X,k}; \tilde{Y}_k | X_{A,k}, X_{k-1}). \quad (159)$$

Define $\tilde{\Phi}_{Y,k} \equiv \angle \tilde{Y}_k$ and

$$q_{\tilde{\Phi}_Y | \Phi_X}(\phi_y | \phi_x) \equiv \frac{\exp(\alpha \cos(\phi_y - \phi_x))}{2\pi I_0(\alpha)}. \quad (160)$$

Furthermore, define

$$\begin{aligned} q_{\tilde{\Phi}_{Y,k} | X_{A,k}, X_{k-1}}(\phi_y | |x_k|, x_{k-1}) \\ &\equiv \int_{-\pi}^{\pi} p_{\Phi_{X,k} | X_{A,k}, X_{k-1}}(\phi_x | |x_k|, x_{k-1}) q_{\tilde{\Phi}_Y | \Phi_X}(\phi_y | \phi_x) d\phi_x \\ &= \frac{1}{2\pi}. \end{aligned} \quad (161)$$

The last equality holds because X_1, \dots, X_n are statistically independent and $\Phi_{X,k}$ is independent of $X_{A,k}$ with a uniform distribution on $[-\pi, \pi)$. We have

$$\begin{aligned} I(\Phi_{X,k}; \tilde{Y}_k | X_{A,k}, X_{k-1}) \\ &\stackrel{(a)}{\geq} I(\Phi_{X,k}; \tilde{\Phi}_{Y,k} | X_{A,k}, X_{k-1}) \\ &\stackrel{(b)}{\geq} \mathbb{E} \left[\log q_{\tilde{\Phi}_Y | \Phi_X}(\tilde{\Phi}_{Y,k} | \Phi_{X,k}) \right] \\ &\quad - \mathbb{E} \left[\log q_{\tilde{\Phi}_{Y,k} | X_{A,k}, X_{k-1}}(\tilde{\Phi}_{Y,k} | |X_k|, X_{k-1}) \right] \\ &\stackrel{(c)}{=} \log(2\pi) - \log(2\pi I_0(\alpha)) + \alpha \mathbb{E} \left[\cos(\tilde{\Phi}_{Y,k} - \Phi_{X,k}) \right] \\ &= -\log(I_0(\alpha)) + \alpha \mathbb{E} \left[\cos(\tilde{\Phi}_{Y,k} - \Phi_{X,k}) \right] \\ &\stackrel{(d)}{\geq} \frac{1}{2} \log \alpha - \alpha + \alpha \mathbb{E} \left[\cos(\tilde{\Phi}_{Y,k} - \Phi_{X,k}) \right] \\ &\geq \frac{1}{2} \log \alpha - \alpha \frac{\sigma_W^2}{2} - \frac{4\alpha}{\text{SNR}\Delta} \end{aligned} \quad (162)$$

where (a) follows from the data processing inequality, (b) follows by extending the result of the auxiliary-channel lower bound theorem in [11, Sec. VI], (c) follows from (160) and

(161), (d) follows from (147) and the last inequality holds because

$$\mathbb{E} \left[\cos(\tilde{\Phi}_{Y,k} - \Phi_{X,k}) \right] \geq 1 - \frac{\sigma_W^2}{2} - \frac{4}{\text{SNR}\Delta} \quad (163)$$

for $\text{SNR}\Delta > 2$, as we will show. Define

$$S_k \equiv 1 + \tilde{Z}_k \quad (164)$$

$$\hat{Y}_k \equiv |X_k| \sqrt{\Delta} e^{j\Phi_{X,k}} + \tilde{N}_k. \quad (165)$$

Therefore, we have

$$\begin{aligned} & \mathbb{E} \left[\cos(\tilde{\Phi}_{Y,k} - \Phi_{X,k}) \right] \\ & \stackrel{(a)}{=} \mathbb{E} \left[\cos(W_{(k-1)L+1} + \Phi_{S,k-1} + \hat{\Phi}_{Y,k} - \Phi_{X,k}) \right] \\ & \stackrel{(b)}{=} \mathbb{E} \left[\cos(W_{(k-1)L+1} + \Phi_{S,k-1}) \right] \mathbb{E} \left[\cos(\hat{\Phi}_{Y,k} - \Phi_{X,k}) \right] \\ & \quad - \mathbb{E} \left[\sin(W_{(k-1)L+1} + \Phi_{S,k-1}) \right] \mathbb{E} \left[\sin(\hat{\Phi}_{Y,k} - \Phi_{X,k}) \right] \end{aligned} \quad (166)$$

where $\Phi_{S,k} \equiv \angle S_k$ and $\hat{\Phi}_{Y,k} \equiv \angle \hat{Y}_k$. Step (a) follows from (156) while step (b) follows from the trigonometric relation $\cos(A+B) = \cos(A)\cos(B) - \sin(A)\sin(B)$ and that $W_{(k-1)L+1} + \Phi_{S,k-1}$ is independent of $\hat{\Phi}_{Y,k}$ and $\Phi_{X,k}$.

Given $X_{A,k} = |x_k|$, \hat{Y}_k is statistically the same as Y in (125) with $R = |x_k| \sqrt{\Delta}$, and therefore we have from Lemma 2 that

$$\mathbb{E} \left[\cos(\hat{\Phi}_{Y,k} - \Phi_{X,k}) \middle| X_{A,k} = |x_k| \right] \geq 1 - \frac{1}{|x_k|^2 \Delta} \quad (167)$$

$$\mathbb{E} \left[\sin(\hat{\Phi}_{Y,k} - \Phi_{X,k}) \middle| X_{A,k} = |x_k| \right] = 0. \quad (168)$$

Equations (166) and (168) imply that we do not need to compute $\mathbb{E} \left[\sin(W_{(k-1)L+1} + \Phi_{S,k-1}) \right]$. We have

$$\begin{aligned} & \mathbb{E} \left[\cos(W_{(k-1)L+1} + \Phi_{S,k-1}) \right] \\ & = \mathbb{E} \left[\cos(W_{(k-1)L+1}) \right] \mathbb{E} \left[\cos(\Phi_{S,k-1}) \right] \\ & \quad - \mathbb{E} \left[\sin(W_{(k-1)L+1}) \right] \mathbb{E} \left[\sin(\Phi_{S,k-1}) \right] \end{aligned} \quad (169)$$

because $W_{(k-1)L+1}$ and $\Phi_{S,k-1}$ are independent. Since $W_{(k-1)L+1}$ is Gaussian with mean 0 and variance $\sigma_W^2 = 2\pi\beta\Delta$, the characteristic function of $W_{(k-1)L+1}$ is

$$\mathbb{E} \left[e^{jW_{(k-1)L+1}} \right] = e^{-\sigma_W^2/2} \quad (170)$$

and by using the linearity of expectation, we have

$$\mathbb{E} \left[\cos(W_{(k-1)L+1}) \right] = \Re \left[\mathbb{E} \left[e^{jW_{(k-1)L+1}} \right] \right] = e^{-\sigma_W^2/2} \quad (171)$$

$$\mathbb{E} \left[\sin(W_{(k-1)L+1}) \right] = \Im \left[\mathbb{E} \left[e^{jW_{(k-1)L+1}} \right] \right] = 0 \quad (172)$$

where $\Re[\cdot]$ and $\Im[\cdot]$ denote the real and imaginary parts, respectively.

Given $X_{k-1} = x_{k-1}$, S_{k-1} is distributed as Y in (125) with $R = |x_{k-1}| \sqrt{\Delta}$. By using Lemma 2, we have

$$\mathbb{E} \left[\cos(\Phi_{S,k-1}) \middle| X_{k-1} = x_{k-1} \right] \geq 1 - \frac{1}{|x_{k-1}|^2 \Delta}. \quad (173)$$

It follows from (169), (171), (172) and (173) that

$$\begin{aligned} & \mathbb{E} \left[\cos(W_{(k-1)L+1} + \Phi_{S,k-1}) \right] \\ & \geq e^{-\sigma_W^2/2} \left(1 - \mathbb{E} \left[\frac{1}{|X_{k-1}|^2} \right] \frac{1}{\Delta} \right). \end{aligned} \quad (174)$$

By combining (166), (167), (168) (174), we have (for $P\Delta > 2$)

$$\begin{aligned} & \mathbb{E} \left[\cos(\tilde{\Phi}_{Y,k} - \Phi_{X,k}) \right] \\ & \geq e^{-\sigma_W^2/2} \left(1 - \mathbb{E} \left[\frac{1}{|X_{k-1}|^2} \right] \frac{1}{\Delta} \right) \left(1 - \mathbb{E} \left[\frac{1}{|X_k|^2} \right] \frac{1}{\Delta} \right) \\ & \stackrel{(a)}{\geq} e^{-\sigma_W^2/2} \left(1 - \frac{2}{P\Delta} \right)^2 \\ & \stackrel{(b)}{\geq} e^{-\sigma_W^2/2} - \frac{4}{P\Delta} \\ & \stackrel{(c)}{\geq} 1 - \frac{\sigma_W^2}{2} - \frac{4}{P\Delta} \end{aligned} \quad (175)$$

where (a) holds because $|X_k|^2 \geq P/2$ and $|X_{k-1}|^2 \geq P/2$, while (b) follows from $e^{-\sigma_W^2/2} \leq 1$ and the non-negativity of $4/(P\Delta)^2$ and (c) follows from $e^{-x} \geq 1 - x$.

It follows from (150), (159) and (162) that

$$\frac{1}{b} I(\Phi_X^b; \mathbf{Y}^b | X_A^b) \geq \frac{b-1}{b} \left[\frac{1}{2} \log \alpha - \alpha\pi\beta\Delta - \frac{4\alpha}{\text{SNR}\Delta} \right]. \quad (176)$$

Hence, we have

$$\begin{aligned} I(\Phi_X; \mathbf{Y} | X_A) & = \lim_{b \rightarrow \infty} \frac{1}{b} I(\Phi_X^b; \mathbf{Y}^b | X_A^b) \\ & \geq \frac{1}{2} \log \alpha - \alpha\pi\beta\Delta - \frac{4\alpha}{\text{SNR}\Delta}. \end{aligned} \quad (177)$$

Setting $\alpha = \text{SNR}\Delta$ (the signal-to-noise ratio in one *sample*) gives

$$I(\Phi_X; \mathbf{Y} | X_A) \geq \frac{1}{2} \log \text{SNR}\Delta - \pi\beta\text{SNR}\Delta^2 - 4. \quad (178)$$

Choosing $L = \lceil \beta\sqrt{\text{SNR}} \rceil$ as in (76) and using $\Delta = 1/L$, we have

$$\lim_{\text{SNR} \rightarrow \infty} \sqrt{\text{SNR}}\Delta = \frac{1}{\beta} \text{ and } \lim_{\text{SNR} \rightarrow \infty} \text{SNR}\Delta^2 = \frac{1}{\beta^2}. \quad (179)$$

Therefore, by taking the limit of SNR tending to infinity, we have

$$\lim_{\text{SNR} \rightarrow \infty} I(\Phi_X; \mathbf{Y} | X_A) - \frac{1}{4} \log \text{SNR} \geq \log \frac{1}{\beta} - \frac{\pi}{\beta} - 4. \quad (180)$$

The last equation implies that phase modulation contributes 1/4 to the pre-log of the information rate. We remark that, since the lower bound (177) is valid for any $\alpha > 0$, one can optimize over α to get the tightest lower bound as follows

$$\begin{aligned} I(\Phi_X; \mathbf{Y} | X_A) & \geq \max_{\alpha > 0} \frac{1}{2} \log \alpha - \alpha \left(\pi\beta\Delta + \frac{4}{\text{SNR}\Delta} \right) \\ & = \frac{1}{2} \log \frac{1}{2\pi\beta\Delta + \frac{8}{\text{SNR}\Delta}} - \frac{1}{2} \\ & = \frac{1}{2} \log \frac{\text{SNR}\Delta}{2\pi\beta\text{SNR}\Delta^2 + 8} - \frac{1}{2}. \end{aligned} \quad (181)$$

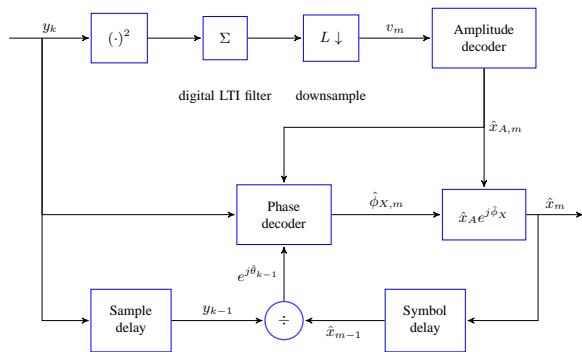


Fig. 12. Two-stage decoding in a multi-sample receiver. The upper branch is part of the double filtering receiver for amplitude decoding. The lower branch is a phase-noise tracker which outputs an estimate $\hat{\theta}_{k-1}$ of the phase noise where $\hat{\theta}_{k-1} = \arg(y_{k-1}/\hat{x}_{m-1})$ where $m = \lceil k/L \rceil$ (cf. (151)). The phase decoder uses the estimate of the phase noise $\hat{\theta}_{k-1}$ and the estimated amplitude $\hat{x}_{A,m}$ to produce an estimate $\hat{\phi}_{X,m}$ of the phase of x_m .

For $L = \lceil \beta\sqrt{\text{SNR}} \rceil$, we have from (179) and (181)

$$\lim_{\text{SNR} \rightarrow \infty} I(\Phi_X; \mathbf{Y}|X_A) - \frac{1}{4} \log \text{SNR} \geq -\log \beta(2\pi + 8\beta) - \frac{1}{2}. \quad (182)$$

We find that the optimum α (the α that gives the tightest lower bound) does not yield a pre-log better than that of $\alpha = \text{SNR}\Delta$.

The main result of this section is summarized in Theorem 4.

Theorem 4: Consider the discrete-time model in (124). If $L = \lceil \beta\sqrt{\text{SNR}} \rceil$ and the input X^n is i.i.d. with $\arg(X_k)$ independent of $|X_k|$ for $k = 1, \dots, n$ such that $\arg(X_k)$ is uniformly distributed over $[-\pi, \pi)$ and $(|X_k|^2 - P/2)$ is exponentially distributed with mean $P/2$, then

$$\lim_{\text{SNR} \rightarrow \infty} I(X_A; \mathbf{Y}) - \frac{1}{2} \log \text{SNR} \geq -2 - \frac{1}{2} \log(8\pi) \quad (183)$$

and

$$\lim_{\text{SNR} \rightarrow \infty} I(\Phi_X; \mathbf{Y}|X_A) - \frac{1}{4} \log \text{SNR} \geq \log \frac{1}{\beta} - \frac{\pi}{\beta} - 4. \quad (184)$$

Moreover, (184) and (183) are achieved by the receiver structure shown in Fig. 12.

The proof of (183) is similar to the proof in Sec. IV-A for the full model and hence the proof is omitted.² As a corollary of Theorem 4, the capacity pre-log for the approximate model (124) satisfies

$$\lim_{\text{SNR} \rightarrow \infty} \frac{C(\text{SNR})}{\log \text{SNR}} \geq \frac{3}{4}. \quad (185)$$

The corollary follows from Theorem 4 by using $C(\text{SNR}) \geq I(X; \mathbf{Y}) = I(X_A; \mathbf{Y}) + I(\Phi_X; \mathbf{Y}|X_A)$. This shows that the capacity grows logarithmically at high SNR with a pre-log factor of at least 3/4.

It is worth pointing out that the phase modulation pre-log of 1/4 requires only 2 samples per symbol for which the time

² The inequality (75) is valid for the approximate model except that G is set to 1, because $F_k = 1$ in the approximate model. Hence, the term $-\pi^2/36$ in (83) does not appear in (183).

TABLE I
ASYMPTOTIC CAPACITY

Model	Baud Rate Sampling ($L = 1$) $C(\text{SNR})$
Without Filtering (15)	$(1/2) \log \text{SNR}$ [8]
With Filtering (13)	$\log \log \text{SNR}$ (conjecture)

TABLE II
ASYMPTOTIC ACHIEVABLE RATE

Model	Oversampling	
	Amplitude Mod. $I(X_A; \mathbf{Y})$	Phase Mod. $I(\Phi_X; \mathbf{Y} X_A)$
Without Filtering (124)	$(1/2) \log \text{SNR}$ [24]	$\geq (1/4) \log \text{SNR}$ [26]
With Filtering (18)	$(1/2) \log \text{SNR}$ [24]	$\geq (1/4) \log \text{SNR}$ [48]

resolution, $1/\Delta$, grows as the square root of the SNR. It is interesting to contemplate whether another receiver, e.g., a non-coherent receiver, can achieve the maximum amplitude modulation pre-log of 1/2 but requires only 1 sample per symbol. If so, one would need only 3 samples per symbol to achieve a pre-log of 3/4.

VIII. SUMMARY AND OPEN PROBLEMS

The known results at high SNR are summarized in Tables I and II. The conjecture in Table I is based on our belief that $\{H_k\}$ in (14) is stationary, ergodic and regular, i.e., its "present" cannot be predicted precisely from its "past" [47]. If this is true, it follows that the capacity grows double-logarithmically with SNR according to Lapidoth and Moser [23]. For the model *without* filtering, it is not known whether phase modulation with oversampling can achieve a pre-log greater than 1/4. For the model *with* filtering, Barletta and Kramer [48] recently showed that phase modulation with oversampling also achieves a pre-log of at least 1/4; we do not know if more is possible. It is worth mentioning that the results in [24] and [26] were obtained by letting the number of samples L per symbols grow with SNR:

$$L = \lceil \beta\sqrt{\text{SNR}} \rceil. \quad (186)$$

However, this is not necessarily the optimum (minimum) oversampling factor to achieve the aforementioned pre-logs. For the model with filtering, we indeed showed in Sec. IV that a pre-log of 1/2 can be achieved using

$$L = \lceil \beta\sqrt[3]{\text{SNR}} \rceil \quad (187)$$

but it is not clear whether this is optimal. For the model without filtering, Barletta and Kramer [49] showed that if

$$L = \lceil \text{SNR}^\alpha \rceil \quad (188)$$

where $0 < \alpha \leq 1$, then the capacity pre-log is at most $(1 + \alpha)/2$ which implies that $L \propto \sqrt{\text{SNR}}$ is optimal for achieving a pre-log of 3/4. The impact of oversampling on the capacity of non-Wiener phase noise channels, or multi-input multi-output (MIMO) phase noise channels, are also interesting open problems.

IX. CONCLUSION

We studied a waveform channel impaired by Wiener phase noise and AWGN. A discrete-time channel model based on filtering and oversampling was derived. The model accounts for the filtering effects on the phase noise. It is shown that, at high SNR, the multi-sample receiver achieves rates that grow logarithmically with SNR with at least a 1/2 pre-log factor, if the number of samples per symbol grows with the cubic root of the SNR. In addition, we computed via numerical simulations lower bounds on the information rates achieved by the multi-sample receiver. We observed that the required oversampling rate depends on the linewidth of the phase noise, the shape of the transmit-pulse and the signal-to-noise ratio. The results demonstrate that multi-sample receivers increase the information rate for both strong and weak phase noise at high SNR. We compared our results with the results obtained by using other discrete-time models. Finally, we showed for an approximate discrete-time model of the multi-sample receiver that phase modulation achieves a pre-log of at least 1/4 while amplitude modulation achieves a pre-log of 1/2, if the number of samples per symbol grows with the square root of the SNR. Thus, we demonstrated that the overall capacity pre-log is 3/4 which is greater than the capacity pre-log of the (approximate) discrete-time Wiener phase noise channel with only one sample per symbol.

APPENDIX A

Appendix A.1

- Wiener process:

The Wiener process $\Theta(t)$ is a Gaussian process with the second-order statistics [50, Sec. 3.8.1]

$$\begin{aligned}\mathbb{E}[\Theta(t) - \Theta(0)] &= 0 \\ \mathbb{E}[(\Theta(t_1) - \Theta(0))(\Theta(t_2) - \Theta(0))] &= 2\pi\beta \min\{t_1, t_2\}.\end{aligned}\quad (189)$$

Property 5: The Wiener process has independent increments, i.e., increments over disjoint time intervals are independent.

Property 6: An increment $\Theta(t_2) - \Theta(t_1)$ is Gaussian with

$$\text{Var}(\Theta(t_2) - \Theta(t_1)) = 2\pi\beta|t_2 - t_1|. \quad (190)$$

- The process $\{F_k\}$

Remark 7: The process $\{F_k\}$ is an i.i.d. process (if the pulse is rectangular).

Proof: The independence follows from Property 5 and because functions of independent random variables are also independent. The identical distribution property follows from the rectangular pulse shape³ and that the integrations are over increments of a Wiener process with equal length. ■

³ If the pulse is not rectangular, the process $\{F_k\}$ is not identically distributed because the phase noise $e^{j\Theta(t)}$ is weighted in a given sample interval according to the pulse shape.

Appendix A.2

- Moments of Gaussian random variables:

Remark 8: If $X \sim \mathcal{N}_{\mathbb{R}}(0, \sigma^2)$, then $\mathbb{E}[X^4] = 3\sigma^4$.

Remark 9: If $Z \sim \mathcal{N}_{\mathbb{C}}(0, \sigma^2)$, then $\mathbb{E}[|Z|^4] = 2\sigma^4$.

Remark 10: If $Z \sim \mathcal{N}_{\mathbb{C}}(0, \sigma^2)$, then $\mathbb{E}[Z|Z|^2] = 0$.

Remark 8 follows from [51, eq (4.54)] while remarks 9 and 10 follow from [51, eq (8.117)].

- $\mathbb{E}[Z_1] = 0$

$$\begin{aligned}\mathbb{E}[Z_1] &\stackrel{(a)}{=} \mathbb{E}\left[\sum_{\ell=1}^L \Re[e^{j\Phi_X} e^{j\Theta_\ell} F_\ell N_\ell^*]\right] \\ &\stackrel{(b)}{=} \sum_{\ell=1}^L \Re[\mathbb{E}[e^{j\Phi_X} e^{j\Theta_\ell} F_\ell] \mathbb{E}[N_\ell^*]] \\ &\stackrel{(c)}{=} 0\end{aligned}\quad (191)$$

Step (a) follows from the definition (43), (b) follows because $\{N_k\}$ is independent of Φ_X , $\{\Theta_k\}$ and $\{F_k\}$, and (c) follows from (21).

- $\mathbb{E}[Z_1^2] = \mathbb{E}[G]\sigma_N^2\Delta L/2$

$$\begin{aligned}\mathbb{E}[Z_1^2] &\stackrel{(a)}{=} \mathbb{E}\left[\sum_{\ell=1}^L \sum_{k=1}^L \Re[e^{j\Phi_X} e^{j\Theta_\ell} F_\ell N_\ell^*] \Re[e^{j\Phi_X} e^{j\Theta_k} F_k N_k^*]\right] \\ &\stackrel{(b)}{=} \mathbb{E}\left[\sum_{\ell=1}^L \sum_{k=1}^L \frac{1}{2} \Re[e^{-j2\Phi_X} e^{-j\Theta_\ell - j\Theta_k} F_\ell^* F_k^* N_\ell N_k + e^{j\Theta_\ell - j\Theta_k} F_\ell F_k^* N_\ell^* N_k]\right] \\ &\stackrel{(c)}{=} \sum_{\ell=1}^L \sum_{k=1}^L \frac{1}{2} \Re\left[\mathbb{E}[e^{-j2\Phi_X} e^{-j\Theta_\ell - j\Theta_k} F_\ell^* F_k^* N_\ell N_k] + \mathbb{E}[e^{j\Theta_\ell - j\Theta_k} F_\ell F_k^* N_\ell^* N_k]\right] \\ &\stackrel{(d)}{=} \sum_{\ell=1}^L \sum_{k=1}^L \frac{1}{2} \Re\left[\mathbb{E}[e^{-j2\Phi_X} e^{-j\Theta_\ell - j\Theta_k} F_\ell^* F_k^*] \mathbb{E}[N_\ell N_k] + \mathbb{E}[e^{j\Theta_\ell - j\Theta_k} F_\ell F_k^*] \mathbb{E}[N_\ell^* N_k]\right] \\ &\stackrel{(e)}{=} \frac{1}{2} \sigma_N^2 \Delta \sum_{\ell=1}^L \mathbb{E}[|F_\ell|^2] \\ &\stackrel{(f)}{=} \frac{1}{2} \sigma_N^2 \Delta L \mathbb{E}[G]\end{aligned}\quad (192)$$

Step (a) follows from the definition (43), (b) follows by using the relation $\Re[A]\Re[B] = \frac{1}{2}\Re[AB + AB^*] = \frac{1}{2}\Re[A^*B^* + A^*B]$, (c) follows from the linearity of the expectation, (d) follows because $\{N_k\}$ is independent of Φ_X , $\{\Theta_k\}$ and $\{F_k\}$, (e) follows from (22) and (23), and (f) follows from (42).

- $\mathbb{E}[Z_0] = \sigma_N^2\Delta L$

$$\begin{aligned}\mathbb{E}[Z_0] &\stackrel{(a)}{=} \mathbb{E}\left[\sum_{\ell=1}^L |N_\ell|^2\right] \\ &\stackrel{(b)}{=} \sigma_N^2\Delta L\end{aligned}\quad (193)$$

Step (a) follows from the definition (44) and (b) follows from (22).

- $\mathbb{E} [(Z_0 - \mathbb{E}[Z_0])^2] = \sigma_N^4 \Delta^2 L$

$$\begin{aligned}
\mathbb{E} [(Z_0 - \mathbb{E}[Z_0])^2] &= \text{Var}(Z_0) \\
&\stackrel{(a)}{=} L \text{Var}(|N_1|^2) \\
&= L(\mathbb{E}[|N_1|^4] - \mathbb{E}^2[|N_1|^2]) \\
&\stackrel{(b)}{=} L(2\sigma_N^4 \Delta^2 - \sigma_N^4 \Delta^2) \\
&= \sigma_N^4 \Delta^2 L \tag{194}
\end{aligned}$$

where (a) holds because $\{N_k\}$ is i.i.d. and (b) follows from Remark 9.

- $\mathbb{E}[Z_1 Z_0] = 0$

$$\begin{aligned}
\mathbb{E}[Z_1 Z_0] &\stackrel{(a)}{=} \mathbb{E} \left[\left[\sum_{\ell=1}^L \Re[e^{j\Phi_X} e^{j\Theta_\ell} F_\ell N_\ell^*] \right] \left[\sum_{k=1}^L |N_k|^2 \right] \right] \\
&\stackrel{(b)}{=} \sum_{\ell=1}^L \sum_{k=1}^L \Re \left[\mathbb{E}[e^{j\Phi_X} e^{j\Theta_\ell} F_\ell] \mathbb{E}[N_\ell^* |N_k|^2] \right] \\
&\stackrel{(c)}{=} \sum_{\ell=1}^L \Re \left[\mathbb{E}[e^{j\Phi_X} e^{j\Theta_\ell} F_\ell] \mathbb{E}[N_\ell^* |N_\ell|^2] \right] \\
&\stackrel{(d)}{=} 0 \tag{195}
\end{aligned}$$

Step (a) follows from the definitions (43) and (44), (b) follows because $\{N_k\}$ is independent of Φ_X , $\{\Theta_k\}$ and $\{F_k\}$, (c) follows from the independence of N_ℓ and N_k for $k \neq \ell$ and (21), i.e., $\mathbb{E}[N_\ell^* |N_k|^2] = \mathbb{E}[N_\ell^*] \mathbb{E}[|N_k|^2] = 0$ for $k \neq \ell$, (d) follows by using Remark 10.

- $\mathbb{E}[Z_1(Z_0 - \mathbb{E}[Z_0])] = 0$
Follows by using (195) and (191).
- $\mathbb{E}[GZ_1] = 0$

$$\begin{aligned}
\mathbb{E}[GZ_1] &\stackrel{(a)}{=} \mathbb{E} \left[\left[\sum_{\ell=1}^L \Re[e^{j\Phi_X} e^{j\Theta_\ell} F_\ell N_\ell^*] \right] \left[\frac{1}{L} \sum_{k=1}^L |F_k|^2 \right] \right] \\
&\stackrel{(b)}{=} \frac{1}{L} \sum_{\ell=1}^L \sum_{k=1}^L \Re \left[\mathbb{E}[e^{j\Phi_X} e^{j\Theta_\ell} F_\ell |F_k|^2] \mathbb{E}[N_\ell^*] \right] \\
&\stackrel{(c)}{=} 0 \tag{196}
\end{aligned}$$

Step (a) follows from the definitions (42) and (43), (b) follows because $\{N_k\}$ is independent of Φ_X , $\{\Theta_k\}$ and $\{F_k\}$, (c) follows from (21).

- $\mathbb{E}[(G-1)Z_1] = 0$
Follows by using (196) and (191).

Appendix A.3

- Details for computing $\mathbb{E}[|F_1|^2]$

Using the definition in (30), we have

$$\begin{aligned}
\mathbb{E}[|F_1|^2] &= \mathbb{E} \left[\frac{1}{\Delta^2} \int_0^\Delta \int_0^\Delta e^{j(\Theta(t_2) - \Theta(t_1))} dt_2 dt_1 \right] \\
&\stackrel{(a)}{=} \frac{1}{\Delta^2} \int_0^\Delta \int_0^\Delta \mathbb{E} \left[e^{j(\Theta(t_2) - \Theta(t_1))} \right] dt_2 dt_1 \\
&\stackrel{(b)}{=} \frac{1}{\Delta^2} \int_0^\Delta \int_0^\Delta e^{-\text{Var}(\Theta(t_2) - \Theta(t_1))/2} dt_2 dt_1 \\
&\stackrel{(c)}{=} \frac{1}{\Delta^2} \int_0^\Delta \int_0^\Delta e^{-\pi\beta\Delta|t_2 - t_1|} dt_2 dt_1 \\
&\stackrel{(d)}{=} \int_0^1 \int_0^1 a^{|u_2 - u_1|} du_2 du_1. \tag{197}
\end{aligned}$$

Step (a) follows from the linearity of expectation, (b) follows by using the characteristic function of a Gaussian random variable [52], (c) follows from (189), and (d) follows from the transformation of variables $t_1 = u_1 \Delta$ and $t_2 = u_2 \Delta$. We define

$$a \equiv e^{-\pi\beta\Delta}. \tag{198}$$

Finally, we have

$$\mathbb{E}[|F_1|^2] = 2 \frac{a - 1 - \log a}{(\log a)^2} \tag{199}$$

by using (197) and the following lemma.

Lemma 11:

$$\int_0^1 \int_0^1 a^{|t-s|} ds dt = 2 \frac{a - 1 - \log a}{(\log a)^2}, \text{ for } a > 0.$$

Proof: Follows by direct integration. \blacksquare

- Details for computing $\mathbb{E}[|F_1|^4]$

We remark that a formula for computing moments of filtered Wiener phase noise (specifically, $\mathbb{E}[|F_1|^{2k}]$ where k is a positive integer) is found in [53]. We proceed to compute $\mathbb{E}[|F_1|^4]$. Let $\mathcal{T} = \{\mathbf{t} : 0 \leq t_i \leq \Delta, i = 1, 2, 3, 4\}$ and

$$\Psi(\mathbf{t}) = \Theta(t_4) - \Theta(t_3) + \Theta(t_2) - \Theta(t_1). \tag{200}$$

The variable $\Psi(\mathbf{t})$ is Gaussian. Using the definition (30), we have

$$\begin{aligned}
\mathbb{E}[|F_1|^4] &= \mathbb{E} \left[\frac{1}{\Delta^4} \int_{\mathbf{t} \in \mathcal{T}} e^{j\Psi(\mathbf{t})} dt \right] \\
&= \frac{1}{\Delta^4} \int_{\mathbf{t} \in \mathcal{T}} e^{-\text{Var}(\Psi(\mathbf{t}))/2} dt \tag{201}
\end{aligned}$$

where the last equality follows by using the characteristic function of a Gaussian random variable.

The set \mathcal{T} can be partitioned into 24 subsets based on the order of t_1, t_2, t_3 and t_4 . However, because of the symmetry, we have

$$\mathbb{E}[|F_1|^4] = \frac{1}{\Delta^4} \left[16 \int_{\mathbf{t} \in \mathcal{T}_1} + 8 \int_{\mathbf{t} \in \mathcal{T}_2} \right] e^{-\text{Var}(\Psi(\mathbf{t}))/2} dt \tag{202}$$

where the sets \mathcal{T}_1 and \mathcal{T}_2 are

$$\begin{aligned}
\mathcal{T}_1 &= \{\mathbf{t} : 0 \leq t_1 \leq t_2 \leq t_3 \leq t_4 \leq \Delta\} \\
\mathcal{T}_2 &= \{\mathbf{t} : 0 \leq t_1 \leq t_3 \leq t_2 \leq t_4 \leq \Delta\}. \tag{203}
\end{aligned}$$

In other words, we need to compute the integral over two subsets only rather than 24 subsets.

For $\mathbf{t} \in \mathcal{T}_1$, we have

$$\begin{aligned} \text{Var}(\Psi(\mathbf{t})) &\stackrel{(a)}{=} \text{Var}(\Theta(t_4) - \Theta(t_3)) + \text{Var}(\Theta(t_2) - \Theta(t_1)) \\ &\stackrel{(b)}{=} 2\pi\beta(t_4 - t_3 + t_2 - t_1) \end{aligned} \quad (204)$$

where (a) follows because $\Theta(t_4) - \Theta(t_3)$ and $\Theta(t_2) - \Theta(t_1)$ are increments of a Wiener process over disjoint time intervals and hence they are independent (see Property 5) while (b) follows from Property 6. We compute the first integral

$$\begin{aligned} K_1 &= \frac{1}{\Delta^4} \int_{\mathbf{t} \in \mathcal{T}_1} e^{-\text{Var}(\Psi(\mathbf{t}))/2} d\mathbf{t} \\ &= \int_0^1 \int_{u_1}^1 \int_{u_2}^1 \int_{u_3}^1 a^{u_4 - u_3 + u_2 - u_1} du_4 du_3 du_2 du_1 \\ &= \frac{6 - 6a + 4 \log a + 2a \log a + (\log a)^2}{2(\log a)^4}. \end{aligned} \quad (205)$$

For $\mathbf{t} \in \mathcal{T}_2$, we can rewrite $\Psi(\mathbf{t})$ as

$$\Psi(\mathbf{t}) = (\Theta(t_4) - \Theta(t_2)) + 2(\Theta(t_2) - \Theta(t_3)) + (\Theta(t_3) - \Theta(t_1))$$

and hence, we have

$$\begin{aligned} \text{Var}(\Psi(\mathbf{t})) &\stackrel{(a)}{=} \text{Var}(\Theta(t_4) - \Theta(t_2)) + \text{Var}(2(\Theta(t_2) - \Theta(t_3))) \\ &\quad + \text{Var}(\Theta(t_3) - \Theta(t_1)) \\ &\stackrel{(b)}{=} 2\pi\beta(t_4 - 3t_3 + 3t_2 - t_1). \end{aligned} \quad (206)$$

Step (a) follows because $\Theta(t_4) - \Theta(t_2)$, $\Theta(t_2) - \Theta(t_3)$ and $\Theta(t_3) - \Theta(t_1)$ are increments of a Wiener process over disjoint time intervals and hence they are independent (see Property 5) while (b) follows from Property 6. Next, we compute the second integral

$$\begin{aligned} K_2 &= \frac{1}{\Delta^4} \int_{\mathbf{t} \in \mathcal{T}_2} e^{-\text{Var}(\Psi(\mathbf{t}))/2} d\mathbf{t} \\ &= \int_0^1 \int_{u_1}^1 \int_{u_3}^1 \int_{u_2}^1 a^{u_4 - 3u_3 + 3u_2 - u_1} du_4 du_2 du_3 du_1 \\ &= \frac{-81 + 80a + a^4 - 36 \log a - 48a \log a}{144(\log a)^4}. \end{aligned} \quad (207)$$

By combining (202), (205) and (207), we obtain

$$\begin{aligned} \mathbb{E}[|F_1|^4] &= \frac{783 - 784a + a^4 + (540 + 240a) \log a + 144(\log a)^2}{18(\log a)^4}. \end{aligned} \quad (208)$$

- Computing $\text{Var}(|F_1|^2)$

$$\begin{aligned} \text{Var}(|F_1|^2) &= \mathbb{E}[|F_1|^4] - (\mathbb{E}[|F_1|^2])^2 \\ &= \frac{711 - 640a - 72a^2 + a^4 + 12(33 + 32a) \log a + 72(\log a)^2}{18(\log a)^4} \end{aligned} \quad (209)$$

- Limits

We have

$$\begin{aligned} \lim_{a \rightarrow 1} \text{Var}(|F_1|^2) &= 0, & \lim_{a \rightarrow 1} \frac{\text{Var}(|F_1|^2)}{\log a} &= 0, \\ \lim_{a \rightarrow 1} \frac{\text{Var}(|F_1|^2)}{(\log a)^2} &= \frac{4}{45}, & \lim_{a \rightarrow 1} \frac{\text{Var}(|F_1|^2)}{(\log a)^3} &= \infty \end{aligned} \quad (210)$$

and

$$\begin{aligned} \lim_{a \rightarrow 1} \frac{(\mathbb{E}[|F_1|^2] - 1)^2}{\log a} &= 0, & \lim_{a \rightarrow 1} \frac{(\mathbb{E}[|F_1|^2] - 1)^2}{(\log a)^2} &= \frac{1}{9}, \\ \lim_{a \rightarrow 1} \frac{(\mathbb{E}[|F_1|^2] - 1)^2}{(\log a)^3} &= \infty. \end{aligned} \quad (211)$$

- Computing $\mathbb{E}[F_1]$

$$\begin{aligned} \mathbb{E}[F_1] &= \frac{1}{\Delta} \int_0^\Delta \mathbb{E}[e^{j(\Theta(\tau) - \Theta(0))}] d\tau \\ &= \frac{1}{\Delta} \int_0^\Delta e^{-\pi\beta\tau} d\tau \\ &= \int_0^1 a^u du \\ &= \frac{a - 1}{\log a}. \end{aligned} \quad (212)$$

- Computing $\text{Var}(F_1)$

We have

$$\begin{aligned} \text{Var}(F_1) &\equiv \mathbb{E}[|F_1 - \mathbb{E}[F_1]|^2] \\ &= \mathbb{E}[|F_1|^2] - |\mathbb{E}[F_1]|^2 \\ &= -\frac{3 - 4a + a^2 + 2 \log a}{(\log a)^2} \end{aligned} \quad (213)$$

which follows by using (199) and (212).

- More limits

It follows from (212) and (213) that

$$\lim_{a \rightarrow 0} \mathbb{E}[F_1] = 1 \text{ and } \lim_{a \rightarrow 0} \text{Var}(F_1) = 0 \quad (214)$$

which further imply that

$$\begin{aligned} \lim_{a \rightarrow 1} \mathbb{E}[|F_1 - 1|^2] &= \lim_{a \rightarrow 1} \text{Var}(F_1) + |\mathbb{E}[F_1] - 1|^2 \\ &= \lim_{a \rightarrow 1} \text{Var}(F_1) + \left| \lim_{a \rightarrow 1} \mathbb{E}[F_1] - 1 \right|^2 \\ &= 0. \end{aligned} \quad (215)$$

Appendix A.4

- Moments of G

We have

$$\mathbb{E}[G] = \mathbb{E}\left[\frac{1}{L} \sum_{\ell=1}^L |F_\ell|^2\right] = \frac{1}{L} \sum_{\ell=1}^L \mathbb{E}[|F_\ell|^2] = \mathbb{E}[|F_1|^2] \quad (216)$$

where we used the definition of G in (42) and that F_1, \dots, F_L are identically distributed (see Remark 7).

Moreover, we have

$$\text{Var}(G) = \text{Var}\left(\frac{1}{L} \sum_{\ell=1}^L |F_\ell|^2\right) = \frac{1}{L} \text{Var}(|F_1|^2) \quad (217)$$

where we used the definition of G in (42) and that F_1, \dots, F_L are i.i.d. (see Remark 7).

- G converges to 1 in mean square as $L \rightarrow \infty$
We have

$$\begin{aligned} \mathbb{E}[(G-1)^2] &= \mathbb{E}[(G - \mathbb{E}[G])^2] + (\mathbb{E}[G] - 1)^2 \\ &= \frac{1}{L} \text{Var}(|F_1|^2) + (\mathbb{E}[|F_1|^2] - 1)^2 \end{aligned} \quad (218)$$

which follows from (217) and (216). By using (209) and (199), we have

$$\begin{aligned} \lim_{L \rightarrow \infty} \mathbb{E}[(G-1)^2] \\ &= \lim_{L \rightarrow \infty} \frac{1}{L} \cdot \lim_{a \rightarrow 1} \text{Var}(|F_1|^2) + \left(\lim_{a \rightarrow 1} \mathbb{E}[|F_1|^2] - 1 \right)^2 = 0. \end{aligned} \quad (219)$$

- Limits

Recall from (16) with $T_s = 1$ and from (198) that $L = 1/\Delta$ and $\Delta = -(\log a)/\pi\beta$. Therefore, (217) and (210) imply

$$\begin{aligned} \lim_{\Delta \rightarrow 0} \frac{\text{Var}(G)}{\Delta} &= 0, & \lim_{\Delta \rightarrow 0} \frac{\text{Var}(G)}{\Delta^2} &= 0, \\ \lim_{\Delta \rightarrow 0} \frac{\text{Var}(G)}{\Delta^3} &= \frac{4}{45}(\pi\beta)^2, & \lim_{\Delta \rightarrow 0} \frac{\text{Var}(G)}{\Delta^4} &= \infty \end{aligned} \quad (220)$$

while (216) and (211) imply

$$\begin{aligned} \lim_{\Delta \rightarrow 0} \frac{(\mathbb{E}[G] - 1)^2}{\Delta} &= 0, & \lim_{\Delta \rightarrow 0} \frac{(\mathbb{E}[G] - 1)^2}{\Delta^2} &= \frac{1}{9}(\pi\beta)^2, \\ \lim_{\Delta \rightarrow 0} \frac{(\mathbb{E}[G] - 1)^2}{\Delta^3} &= \infty. \end{aligned} \quad (221)$$

APPENDIX B

- *Lemma 12:* Suppose Φ_X and Φ_Y are real-valued circular⁴ random variables [45]. Suppose $p_{\Phi_Y|\Phi_X}(\cdot|\cdot)$ is a conditional probability density such that $p_{\Phi_Y|\Phi_X}(\phi_y|\phi_x) = p_\Phi(\phi_y - \phi_x)$ and $p_\Phi(\cdot)$ is periodic with a period 2π . Then, for any bounded function $f(\cdot)$ that is periodic with a period 2π , we have

$$\mathbb{E}[f(\Phi_Y - \Phi_X)] = \int_{-\pi}^{\pi} p_\Phi(\phi) f(\phi) d\phi. \quad (222)$$

This implies that $\mathbb{E}[f(\Phi_Y - \Phi_X)]$ does not depend on the distribution of Φ_X .

Proof: First, we remark that the pdf of a circular random variable is defined on the whole real line and is normalized over any interval of length 2π [45, Ch.3], e.g., we have

$$\int_x^{x+2\pi} p_{\Phi_Y|\Phi_X}(\phi_y|\phi_x) d\phi_y = 1, \quad -\infty < x < \infty. \quad (223)$$

⁴ Circular random variables are random variables defined on a circle, i.e., random angles and should not be confused with circularly-symmetric random variables.

We proceed to the proof.

$$\begin{aligned} \mathbb{E}[f(\Phi_Y - \Phi_X)] \\ &= \int_{-\pi}^{\pi} \int_{-\pi}^{\pi} p_{\Phi_X, \Phi_Y}(\phi_x, \phi_y) f(\phi_y - \phi_x) d\phi_y d\phi_x \\ &\stackrel{(a)}{=} \int_{-\pi}^{\pi} p_{\Phi_X}(\phi_x) \int_{-\pi}^{\pi} p_\Phi(\phi_y - \phi_x) f(\phi_y - \phi_x) d\phi_y d\phi_x \\ &\stackrel{(b)}{=} \int_{-\pi}^{\pi} p_{\Phi_X}(\phi_x) \int_{-\pi-\phi_x}^{\pi-\phi_x} p_\Phi(\phi) f(\phi) d\phi d\phi_x \\ &\stackrel{(c)}{=} \int_{-\pi}^{\pi} p_{\Phi_X}(\phi_x) \int_{-\pi}^{\pi} p_\Phi(\phi) f(\phi) d\phi d\phi_x \\ &= \int_{-\pi}^{\pi} p_{\Phi_X}(\phi_x) d\phi_x \int_{-\pi}^{\pi} p_\Phi(\phi) f(\phi) d\phi \\ &= \int_{-\pi}^{\pi} p_\Phi(\phi) f(\phi) d\phi \end{aligned} \quad (224)$$

where (a) follows from the chain rule of probability and because $p_{\Phi_Y|\Phi_X}(\phi_y|\phi_x) = p_\Phi(\phi_y - \phi_x)$, (b) follows from the transformation of variables $\phi = \phi_y - \phi_x$ and (c) holds because $p_\Phi(\phi) f(\phi)$ is periodic with period 2π . ■

- *Lemma 13:* For $z \geq 0$, $\text{erfc}(-z) \geq 2 - e^{-z^2}$.

Proof: Since for any real number z

$$\text{erf}(-z) = -\text{erf}(z) \quad (225)$$

$$\text{erfc}(z) = 1 - \text{erf}(z) \quad (226)$$

we have

$$\text{erfc}(-z) = 1 - \text{erf}(-z) = 1 + \text{erf}(z) = 2 - \text{erfc}(z). \quad (227)$$

To complete the proof, we use [44, eq(5)]

$$\text{erfc}(z) \leq e^{-z^2} \text{ for } z \geq 0. \quad (228)$$

- *Lemma 14:* $\sin t \leq t$ for $t \geq 0$.

Proof: Since $1 - \cos z \geq 0$, then for $t \geq 0$ we have

$$\int_0^t (1 - \cos z) dz \geq 0 \quad (229)$$

which implies that (for $t \geq 0$)

$$t - \sin t \geq 0. \quad (230)$$

- *Lemma 15:* Let $a \geq 0$. Then for $t \geq 0$, we have

$$\cos^2 t e^{-a \sin^2 t} \geq (1 - t^2) e^{-at^2}. \quad (231)$$

Proof: The trigonometric identity $\cos^2 t + \sin^2 t = 1$ and $\sin t \leq t$ (Lemma 14) imply that

$$\cos^2 t \geq 1 - t^2. \quad (232)$$

Since the exponential function is monotone, we further have

$$e^{-a \sin^2 t} \geq e^{-at^2}. \quad (233)$$

By combining the two inequalities, we obtain

$$\cos^2 t e^{-a \sin^2 t} \geq (1 - t^2) e^{-at^2}. \quad (234)$$

- **Lemma 16:** Let $a > 0$ and n be a positive integer. Then we have

$$\max_x x^n e^{-ax^2} = \left(\frac{n}{2ae}\right)^{n/2}. \quad (235)$$

REFERENCES

- [1] A. Demir, A. Mehrotra, and J. Roychowdhury. Phase noise in oscillators: a unifying theory and numerical methods for characterization. *IEEE Trans. on Circ. and Sys. I: Fund. Theory and App.*, vol. 47(no. 5):pp. 655–674, 2000.
- [2] E. Casini, R. D. Gaudenzi, and A. Ginesi. DVB-S2 modem algorithms design and performance over typical satellite channels. *Int. J. on Sat. Comm. and Net.*, vol. 22(no. 3):pp. 281–318, 2004.
- [3] G. Durisi, A. Tarable, and T. Koch. On the multiplexing gain of MIMO microwave backhaul links affected by phase noise. *IEEE Int. Conf. on Comm. (ICC)*, Jun. 2013.
- [4] R.W. Tkach and A.R. Chraplyvy. Phase noise and linewidth in an InGaAsP DFB laser. *J. Lightwave Tech.*, vol. 4(no. 11):pp. 1711–1716, 1986.
- [5] A.J. Viterbi. Phase-locked loop dynamics in the presence of noise by Fokker-Planck techniques. *Proc. IEEE*, vol. 51(no. 12):pp. 1737–1753, 1963.
- [6] M. Katz and S. Shamai. On the capacity-achieving distribution of the discrete-time noncoherent and partially coherent AWGN channels. *IEEE Trans. Inf. Theory*, vol. 50(no. 10):pp. 2257–2270, Oct. 2004.
- [7] P. Hou, B.J. Belzer, and T.R. Fischer. On the capacity of the partially coherent additive white Gaussian noise channel. *IEEE Int. Sym. Inf. Theory (ISIT)*, pages 372–372, Jul. 2003.
- [8] A. Lapidoth. Capacity bounds via duality: A phase noise example. *Asian-European Workshop on Information Theory*, pages 58–61, Jun. 2002.
- [9] J. Dauwels and H.-A. Loeliger. Computation of information rates by particle methods. *IEEE Trans. Inf. Theory*, vol. 54(no. 1):pp. 406–409, Jan. 2008.
- [10] L. Barletta, M. Magarini, and A. Spalvieri. Estimate of information rates of discrete-time first-order Markov phase noise channels. *IEEE Photonics Tech. Letters*, vol. 23(no. 21):pp. 1582–1584, Nov. 2011.
- [11] D.M. Arnold, H.-A. Loeliger, P.O. Vontobel, A. Kavcic, and Wei Zeng. Simulation-based computation of information rates for channels with memory. *IEEE Trans. Inf. Theory*, vol. 52(no. 8):pp. 3498–3508, Aug. 2006.
- [12] L. Barletta, M. Magarini, and A. Spalvieri. The information rate transferred through the discrete-time Wiener’s phase noise channel. *J. Lightwave Tech.*, vol. 30(no. 10):pp. 1480–1486, May 2012.
- [13] L. Barletta, M. Magarini, and A. Spalvieri. A new lower bound below the information rate of Wiener phase noise channel based on Kalman carrier recovery. *Optics Express*, vol. 20(no. 23):pp. 25471–25477, Nov. 2012.
- [14] A. Barbieri and G. Colavolpe. On the information rate and repeat-accumulate code design for phase noise channels. *IEEE Trans. Commun.*, vol. 59(no. 12):pp. 3223–3228, Dec. 2011.
- [15] G. Durisi, A. Tarable, C. Camarda, and G. Montorsi. On the capacity of MIMO Wiener phase-noise channels. *Inf. Theory and App. Workshop (ITA)*, pages 1–7, Feb. 2013.
- [16] G. Durisi, A. Tarable, C. Camarda, R. Devassy, and G. Montorsi. Capacity Bounds for MIMO Microwave Backhaul Links Affected by Phase Noise. *IEEE Trans. Commun.*, vol. 62(no. 3):pp. 920–929, March 2014.
- [17] B. Goebel, R. Essiambre, G. Kramer, P.J. Winzer, and N. Hanik. Calculation of mutual information for partially coherent Gaussian channels with applications to fiber optics. *IEEE Trans. Inf. Theory*, vol. 57(no. 9):pp. 5720–5736, Sep. 2011.
- [18] L. Barletta and G. Kramer. On continuous-time white phase noise channels. *IEEE Int. Sym. Inf. Theory (ISIT)*, 2014.
- [19] L. Barletta and G. Kramer. Signal-to-noise ratio penalties for continuous-time phase noise channels. *Int. Conf. on Cog. Rad. Oriented Wireless Net. (CROWCOM)*, 2014.
- [20] G.J. Foschini and G. Vannucci. Characterizing filtered light waves corrupted by phase noise. *IEEE Trans. Inf. Theory*, vol. 34(no. 6):pp. 1437–1448, Nov. 1988.
- [21] G.J. Foschini, L.J. Greenstein, and G. Vannucci. Noncoherent detection of coherent lightwave signals corrupted by phase noise. *IEEE Trans. Commun.*, vol. 36(no. 3):pp. 306–314, Mar. 1988.
- [22] G.J. Foschini, G. Vannucci, and L.J. Greenstein. Envelope statistics for filtered optical signals corrupted by phase noise. *IEEE Trans. Commun.*, vol. 37(no. 12):pp. 1293–1302, Dec. 1989.
- [23] A. Lapidoth and S.M. Moser. Capacity bounds via duality with applications to multiple-antenna systems on flat-fading channels. *IEEE Trans. Inf. Theory*, vol. 49(no. 10):pp. 2426–2467, Oct. 2003.
- [24] H. Ghozlan and G. Kramer. On Wiener phase noise channels at high signal-to-noise ratio. *IEEE Int. Sym. Inf. Theory (ISIT)*, pages 2279–2283, 2013.
- [25] H. Ghozlan and G. Kramer. Multi-sample receivers increase information rates for wiener phase noise channels. *IEEE Global Telecom. Conf. (GLOBECOM)*, pages 1919–1924, 2013.
- [26] H. Ghozlan and G. Kramer. Phase modulation in Wiener phase noise channels with oversampling at high SNR. *IEEE Int. Sym. Inf. Theory (ISIT)*, 2014.
- [27] R. Pighi and R. Raheli. Information rates of oversampled detectors for transition-noise-limited digital storage systems. *IEEE Int. Sym. Inf. Theory (ISIT)*, pages 2536–2540, 2007.
- [28] E.N. Gilbert. Increased information rate by oversampling. *IEEE Trans. Inf. Theory*, vol. 39(no. 6):pp. 1973–1976, 1993.
- [29] T. Koch and A. Lapidoth. Increased capacity per unit-cost by oversampling. *IEEE Convention of Electrical and Electronics Engineers in Israel (IEEEI)*, pages 684–688, Nov. 2010.
- [30] M. Dörpinghaus, G. Koliander, G. Durisi, E. Riegler, and H. Meyr. Oversampling Increases the Pre-Log of Noncoherent Rayleigh Fading Channels. *IEEE Trans. Inf. Theory*, vol. 60(no. 9):pp. 5673–5681, Sept. 2014.
- [31] S.M. Moser. Capacity results of an optical intensity channel with input-dependent Gaussian noise. *IEEE Trans. Inf. Theory*, vol. 58(no. 1):pp. 207–223, Jan. 2012.
- [32] M. Peleg, S. Shamai, and S. Galan. Iterative decoding for coded noncoherent MPSK communications over phase-noisy AWGN channel. *IEEE Proc. Comm.*, vol. 147(no. 2):pp. 87–95, Apr. 2000.
- [33] A. Barbieri, G. Colavolpe, and G. Caire. Joint iterative detection and decoding in the presence of phase noise and frequency offset. *IEEE Trans. Commun.*, vol. 55(no. 1):pp. 171–179, Jan. 2007.
- [34] A. Spalvieri and L. Barletta. Pilot-aided carrier recovery in the presence of phase noise. *IEEE Trans. Commun.*, vol. 59(no. 7):pp. 1966–1974, Jul. 2011.
- [35] Y.E. Dallah and S. Shamai. An upper bound on the error probability of quadratic-detection in noisy phase channels. *IEEE Trans. Commun.*, vol. 39(no. 11):pp. 1635–1650, Nov. 1991.
- [36] Y.E. Dallah and S. Shamai. Performance bounds for noncoherent detection under Brownian phase noise. *IEEE Trans. Inf. Theory*, vol. 38(no. 2):pp. 362–379, Mar. 1992.
- [37] Y.E. Dallah, G. Jacobsen, and S. Shamai. Analytical upper bounds for noisy phase optical communication invoking Gaussian quadratic functionals. *IEEE Photonics Tech. Letters*, vol. 5(no. 7):pp. 855–858, Jul. 1993.
- [38] Y.E. Dallah and S. Shamai. Coding for DPSK noisy phase channels. *IEEE Trans. Commun.*, vol. 42(no. 234):pp. 927–940, Feb. 1994.
- [39] M. Martalò, C. Tripodi, and R. Raheli. On the information rate of phase noise-limited communications. *Inf. Theory and App. Workshop (ITA)*, 2013.
- [40] N. M. Blachman. A comparison of the informational capacities of amplitude- and phase-modulation communication systems. *Proc. IRE*, vol. 41(no. 6):pp. 748–759, 1953.
- [41] A. D. Wyner. Bounds on communication with polyphase coding. *Bell Sys. Tech. J.*, vol. 45(no. 4):pp. 523–559, April 1966.
- [42] J.P. Aldis and A.G. Burr. The channel capacity of discrete time phase modulation in AWGN. *IEEE Trans. Inf. Theory*, vol. 39(no. 1):pp. 184–185, Jan. 1993.
- [43] I.S. Gradshteyn and I.M. Ryzhik. *Table of integrals, series and products*. Academic Press, 2007.
- [44] M. Chiani and D. Dardari. Improved exponential bounds and approximation for the Q-function with application to average error probability computation. *IEEE Global Telecom. Conf. (GLOBECOM)*, vol. 2:pp. 1399–1402, Nov. 2002.
- [45] Kanti V. Mardia and Peter E. Jupp. *Directional Statistics*. John Wiley and Sons Ltd., 2000.
- [46] H. Ghozlan and G. Kramer. Interference focusing for mitigating cross-phase modulation in a simplified optical fiber model. *IEEE Int. Sym. Inf. Theory (ISIT)*, pages 2033–2037, Jun. 2010.
- [47] A. Lapidoth. On the asymptotic capacity of stationary Gaussian fading channels. *IEEE Trans. Inf. Theory*, 51(2):437–446, Feb. 2005.

- [48] L. Barletta and G. Kramer. Lower bound on the capacity of continuous-time Wiener phase noise channels. *IEEE Int. Sym. Inf. Theory (ISIT)*, 2015.
- [49] L. Barletta and G. Kramer. Upper bound on the capacity of discrete-time Wiener phase noise channels. *IEEE Inf. Theory Workshop (ITW)*, 2015 (pre-print available on arxiv.org).
- [50] C. W. Gardiner. *Handbook of Stochastic Methods: For Physics, Chemistry and Natural Sciences*. Springer, 2nd edition, 1985.
- [51] H. Kobayashi, B.L. Mark, and W. Turin. *Probability, Random Processes, and Statistical Analysis: Applications to Communications, Signal Processing, Queueing Theory and Mathematical Finance*. Cambridge University Press, 2012.
- [52] Athanasios Papoulis and S. Unnikrishna Pillai. *Probability, Random Variables and Stochastic Processes*. McGraw-Hill, 4th edition, 2002.
- [53] Y.E. Dallal and S. Shamai. Power moment derivation for noisy phase lightwave systems. *IEEE Trans. Inf. Theory*, vol. 40(no. 6):pp. 2099–2103, Nov. 1994.